Simulating interactions of fire, climate, and management to characterize the future range of variability in dry forests of the East Cascades

Sofia Saenz Kruszka

A thesis

Submitted in partial fulfillment of the

Requirements for the degree of

Master of Science

University of Washington

2026

Committee:

Brian J. Harvey

Kristin H. Braziunas

Soo-Hyung Kim

Program Authorized to Offer Degree:

Environmental and Forest Sciences

University of Washington

Abstract

Simulating interactions of fire, climate, and management to characterize the future range of variability in dry forests of the East Cascades

Sofia Saenz Kruszka

Chair of the Supervisory Committee:
Brian J. Harvey, Associate Professor
School of Environmental and Forest Sciences

Changing climate and altered disturbance regimes highlight the need for understanding the past, present, and future range of variability of ecosystems and natural disturbances. For many interior dry forests of the western USA, frequent fire (occurring at multi-year to multi-decadal intervals) is an essential disturbance that drives heterogenous forest structure composition and patterns that foster resilience to future wildfire. More than a century of fire suppression and exclusion has increased density, fuel accumulation, and homogenous structure, leaving dry forests vulnerable to drought stress and uncharacteristic amounts of high severity wildfire. The reference range of variability (rRV), or an estimate of forest conditions before management- and land use-driven forest change, is a common guide for locating and quantifying the need for density and fuel reduction treatments in forests that have departed from their historical conditions. However, as compounding effects of climate and land use change alter fire regimes, forest managers need new guideposts for facilitating forest adaptation to future conditions. The future range of variability (FRV) can be a better tool for adaptive management by forecasting the effects of different drivers of forest change—wildfire, climate change, and management—on forest structure at long temporal and broad spatial scales Here, I use the Individual-based Forest Landscape and Disturbance (iLand) model to simulate the FRV of landscape-level forest structure patterns for interior dry forests in the Pacific Northwest under different future wildfire, climate, and management scenarios. We incorporate spatially explicit gridded vegetation, climate, and soils data to simulate emergent outcomes of forest structure, across a 46,000 ha dry forest landscape in the Washington East Cascades over a period of 75 years into the future. Wildfire decreased the cover and continuity of mid-seral closed canopy forests and increased the cover of late seral open canopy forests. Climate change increased the cover of closed canopy forest overall. When fire and climate change were enabled in simulations, adding management reduced the mean percent cover and continuity of mid-seral closed canopy forest. Although wildfire alone reduced the mean cover and continuity of mid-seral closed canopy structure in dry forests, a surplus of mid-seral closed canopy remained on the landscape (33% more than the rRV). Findings from this study demonstrate that wildfire is more effective than management at reducing the cover and continuity of mid-seral closed canopy forest, which is expected and aligns with existing studies of the effects of wildfire on current forest structure restoration need in eastern WA. Comparison of the FRV with the rRV shows that wildfire and management are insufficient for reducing mid-seral closed canopy cover closer to reference ranges in dry forests over the course of the century. Further study is needed to understand how alternative adaptive management strategies influence the FRV of forest structure.

TABLE OF CONTENTS

LIST OF FIGURES

LIST OF TABLES

Acknowledgements

Brian Harvey—*Thank you for your guidance, teaching, and support. You are a model of excellent science and leadership, and I am incredibly lucky to be your mentee. Thank you for building a strong and supportive community in your lab—there's no better place to become an ecologist than here.*

iLand team—*Thank you to Kristin Braziunas and Jenna Morris for teaching me how to be a modeler and a better ecologist at the same time. Your boundless knowledge and expertise are a marvel.*

Harvey Lab—*Thank you for being a supportive and passionate science community. I am so proud to be learning and growing with all of you.*

Collaborators Tom DeMeo, Skye Greenler, and Kerry Kemp—*Thank you for the expertise you have contributed to this project.*

Committee members Kristin H. Braziunas and Soo-Hyung Kim—*thank you for your thoughtful insights and feedback.*

1. Introduction

As climate warming and associated changes to natural disturbance regimes accelerate, so does the need for understanding how natural disturbances influence landscape-level forest dynamics (Halofsky et al., 2014; Haugo et al., 2015). In many forest landscapes across the world, fire is a natural disturbance that drives key dimensions of forest structure, composition, and function. For example, the exclusion and suppression of fire by settler colonial forest management in North America have significantly altered the structure and composition of forests once shaped by frequent fire disturbance (Hessburg et al., 2005). These changes in forest structure were a result of management (e.g., fire suppression, exclusion of fire to reduce surface fuels and understory fuels), but also of altered fire regimes (Halofsky et al., 2020)—the frequency, magnitude, variability, seasonality, and extent of fire disturbances in a system (Agee, 1998). Novel changes in fire regimes may reduce the capacity of forested landscapes to remain resilient, or maintain characteristic structure and function after fire disturbance (Holling, 1973). Future climate change can drive novel disturbance regimes and stress forests to a state of vulnerability to vegetation state transitions (Turner and Seidl, 2023). Increasingly warmer and drier climate conditions leave forests vulnerable to post-fire transition to non-forest after fire due to harsher post-fire conditions and larger high severity patch sizes (Davis et al., 2023; Harvey et al., 2016; Kemp et al., 2019; Meigs et al., 2023). Although understanding the range of historical forest conditions has important implications for restoring resilient forests, projecting the degree to which changes in fire regime, climate and management practices will drive forest change has implications for adaptive management and retaining important ecosystem services into the future.

In western North America, characteristic wildfire size, severity, and return interval for a given wildfire regime yield characteristic patchworks of seral structural classes (structure classifications that reflect the general canopy openness and largest size class of a stand) at landscape (over 46,000 ha) scales (Haugo et al., 2015). Across the Pacific northwest (PNW), several categorical schemes exist to classify forest structure into 5-8 classes based on stand-level characteristics (e.g., canopy cover, canopy layers, tree size classes). See Appendix A.1 for an overview of the classification schemes used by managers in Washington (WADNR 2020). The ‘5-box’ model of structure classifications used by the US Forest Service (Table 1.1 and Table

1.7) uses canopy cover and the quadratic mean diameter of the 25% largest trees in a stand to break forest structure into 1) early-seral, 2) mid-seral closed canopy, 3) mid-seral open canopy, 4) late-seral open canopy, and 5) late-seral closed canopy. Structure class classification models like the 5-box model are tools for quantifying the composition and pattern of forest structure at broad spatial scales (e.g., Hessburg et al., 1999; Haugo et al., 2015; DeMeo et al., 2018; Churchill et al., 2022; Laughlin et al., 2023).

Table 1.1 Structure class schemes across management agencies in Washington (adapted from Table 6 in WADNR, 2020. See Appendix A.1 for full table) and Oregon (Haugo et al., 2015). The 6-box model is applied in the WADNR Forest health treatment summary table (Figure 1.1) and was used to assign management inputs. 'Small', 'Medium', and 'Large' refer to the dominant size class, and 'Open' and 'Dense' refer to the general density of a stand. The 5-box model has been applied to forests across the entire region (i.e., Haugo et al., 2015) and is used in this study to derive gridded structure class outputs. 'Early', 'Mid' and 'Late' refer to the general age, and 'Open' and 'Closed' refer to the canopy cover of a stand.

6-box classes for assigning management inputs	5-box classes for deriving structure class outputs	Definition*
Small Open	Early	CACO < 10% OR DBH < 25.4 cm, CACO >= 10% and < 40%
Small Dense	Early	DBH < 25.4 cm, CACO >= 40%
Medium Open	Mid Open	DBH >= 25.4 cm and < 50.8 cm, CACO >= 10% and < 40%
Medium Dense	Mid Closed	DBH >= 25.4 cm and < 50.8 cm, CACO >= 40%
Large Open	Late Open	DBH >= 50.8 cm, CACO >= 10% and < 40%
Large Dense	Late Closed	DBH >= 50.8 cm, CACO >= 40%

*CACO = canopy cover, DBH = quadratic mean diameter of largest 25% trees

In eastern Washington, more than a century of fire suppression and exclusion has altered forests and fuels. Historically, dry forests in low- to mid-elevations dominated by *Pinus ponderosa* (ponderosa pine) in the canopy and *Pseudotsuga menziesii* (Douglas-fir) in the understory were prone to frequent low severity wildfires (Franklin and Dyrness, 1973). Frequent fires facilitated an open canopy, sparse understory and fuel bed, and a spatially clumped tree distribution (Hessburg et al., 2005). Exclusion of wildfire has increased the cover and connectivity of dense closed canopy forests dominated by shade intolerant species (i.e., Douglas-fir and *Abies grandis* or grand fir) that are less fire-resilient than ponderosa pine, and the homogenization of moist mixed conifer forests dominated by the same species (Johnston, 2017). Further, selective logging of large-diameter fire resistant trees has assisted the overgrowth of mid-seral closed canopy forest and decline of late-seral forests in Washington (Haugo et al., 2015). Departures from historical conditions towards denser, more fuel-abundant forests have potential to increase drought stress and the likelihood of high severity fire events in dry and moist mixed-conifer forests (Churchill et al., 2022).

Characterizing a reference range of variability (rRV) of forests before Euro-American settlement and western forest management has been useful for assessing how forests have changed over the last century in response to climate change and fire suppression and exclusion (Swetnam et al., 1999; Dollinger et al., 2024). The rRV is a reference for understanding how current forest conditions have departed from the historical baseline due to climate change (e.g., D. C. Laughlin et al., 2004), or departures from natural disturbance regimes (e.g., Hessburg et al., 1999; Haugo et al. 2015). The rRV, is also a tool for quantifying how much fire and restoration would return departed forest landscapes to pre-settlement conditions (Haugo et al., 2015; Landres et al., 1999; Laughlin et al., 2023; Rollins, 2009).

Fire and management can aid in restoring dry and moist mixed-conifer forests east of the Cascades in Oregon and Washington closer to the rRV (DeMeo et al., 2018; Haugo et al., 2015; Laughlin et al., 2023). Contemporary management and restoration initiatives, such as the USFS Landscape Investments and Collaborative Forest Landscape Restoration Program (CFLRP), have targeted interior dry forests east of the Cascades for projects aiming to restore landscapes towards historical structural, compositional, and functional targets with fuel reduction treatments (*Confronting the Wildfire Crisis*, 2022; *CFLRP Proposals and Work Plans*, n.d.). Low- and moderate-severity wildfires in dry forests supplement these efforts as well and can often shift conditions to more closely align with the rRV (Churchill et al., 2022; Laughlin et al., 2023).

As climate continues to trend towards warm and dry conditions and fires become less characteristic of the historical fire regime, the rRV becomes a less feasible guidepost for maintaining fire- and climate-adapted forests (Keane et al., 2009). Modeled climate projections and contemporary vegetation maps can help identify potential future ranges of variability (FRV) based on different management and climate change scenarios (Keane et al., 2020, 2019). The

FRV has been applied to projections of vegetation type distributions due to climate and wildfire (Churchill et al., 2022) and future changes in fire regimes (Gaudreau et al., 2016). Thus, quantifying the FRV in ecosystems vulnerable to novel climate and associated fire regimes is equally as important as the rRV for understanding how to manage for maintaining ecosystem structure, composition, and function in the future (Turner and Seidl, 2023).

Simulation models provide an opportunity to mechanistically explore the effects of fire, climate change, and forest management (i.e., density and fuel reduction treatments) on structure, composition, and function of dry forest landscapes within rRV and FRV frameworks. Previous applications of process-based simulation models to explore future long-term effects of climate, fire, and management on vegetation in the PNW have operated at coarse scales (100m-1km) to capture landscape-scale dynamics (e.g., Halofsky et al., 2014; Furniss et al., 2023; Daum et al., 2024). Application of an individual-based process model that simulates mechanistic processes at a fine spatial grain (2m-10m resolution) can reveal how the FRV of fire and forest structure are impacted by the bottom-up effects of management and climate change.

The Individual-based Forest Landscape and Disturbance (iLand) model is a spatially explicit, process-based model that simulates individual tree growth, competition, mortality, and establishment at a fine spatial grain that can scale up to 60k hectares (Seidl et al., 2012a; Turner et al., 2022). Simulation of individual trees (trees > 4 m height), sapling cohorts (trees < 4 m height) and detailed environmental inputs contribute to realistic simulations of complex ecological patterns at broader scales, such as spatial heterogeneity of biological diversity and forest structure (Seidl et al., 2012a). In addition, iLand dynamically simulates fire at a 20m resolution, further contributing to complex simulations of ecological processes (Hansen et al., 2020). Thus, iLand is a useful tool that can simulate key drivers of forest change—fire, climate change, management activities—and complex emergent outcomes of the FRV of forest structure (Dollinger et al., 2024).

To understand how contemporary vegetation structures will change over the course of the century, we simulated wildfire, climate change, and active management on a 46,000 ha landscape for 75 years. We ask: what are the effects of wildfire, climate change, and management on the future range of variability of forest structure composition and pattern across a frequent-fire forest over the next 75 years? How do estimates of the FRV of structure class composition compare with the rRV? We hypothesize that wildfire, the major natural disturbance that shapes interior PNW dry forest structure (Hessburg et al., 2005), will drive the most change in modeled patterns of forest structure in the next century compared to management and climate change. We also predict that fire and management will bring landscape-scale structure class composition closer to the rRV, while climate change will bring structure class composition further from the rRV. In dry and moist mixed conifer forests on the eastern slopes of the Cascades, several forest restoration and fuel mitigation initiatives are underway ("CFLRP Proposals and Work Plans," n.d.; "Confronting the Wildfire Crisis," 2022), making the findings from this study immediately relevant. Additionally, characterizing the FRV of a priority planning area has implications for planning management on other high-priority restoration areas in the PNW.

2. Methods

2.1 Study Area

The Chumstick-Lower Peshastin planning area covers 46,674 hectares of land—34,080 ha are forested—in the eastern slopes of the Cascade mountains in Washington. The planning area covers a diverse range of forest types, dominated by mesic ponderosa pine, dry mixed conifer, and moist mixed conifer, and including areas of xeric *Tsuga mertensiana* (mountain hemlock), low elevation *Abies amabilis* (Pacific silver fir), and subalpine woodland (see Appendix A.2 for a breakdown of these types across the landscape). The focal landscape is made up of five hydrologic unit code 12 (HUC12) sub watersheds that vary in forest type composition, land ownership composition, and management objectives (Figure 1.2. See Appendix A.2 for details).

The focal landscape has been identified by public land management agencies as in need of fire risk reduction and forest health management due to: large areas of dry forest that are structurally departed and vulnerable to high severity wildfire, a high amount of public land adjacent to the wildland urban interface, and large and continuous areas of suburban development that would benefit from fuel reduction management in surrounding forested areas (Richmond, 2024). The focal landscape is a Washington Department of Natural Resources (WA

DNR) priority landscape, which has been evaluated and prioritized for management need as a part of the DNR 20-year Forest Health Strategic Plan (Figures 1.1 and 1.2) ("20-Year Forest Health Strategic Plan: Eastern Washington | Department of Natural Resources," n.d.). Additionally, this landscape overlaps with two relevant US Forest Service restoration initiatives currently in motion: the Wildfire Crisis Strategy (WCS) and the North Central Washington CFLRP (Figure 1.2) ("CFLRP Proposals and Work Plans," n.d.; "Confronting the Wildfire Crisis," 2022). Thus, this focal landscape is representative of the historically fire-adapted and structurally departed forest types that this study's research questions aim to explore.

Forest conditions to treat		Treatment need (acres)	Current acres by major landowner*				
Type	Size class		USFS	Private	Industrial	DNR-Trust	Other
Dry Dense	Small	500 - 1,500	2,739	838	2,200	745	231
	Medium-Large	21,000 - 25,500	17,423	8,483	2,331	1,255	1,266
Moist Dense	Small	750 - 1,250	2,799	393	1,529	277	0
	Medium-Large	4,000 - 8,250	13,328	1,351	971	735	0
Dry + Moist Open	Medium-Large	10,250 - 16,500	11,780	7,446	2,668	500	313
Total		**36,500 - 53,000**	**These are current acres, not targets*				
Anticipated treatment type	(light blue)	Noncommercial thin plus fuels treatment. May be fire only (prescribed or managed wildfire).					
	(blue)	Commercial thin plus fuels treatment if access exists. May be noncommercial, fire only (prescribed or managed wildfire), or regeneration treatment.					
	(green)	Maintenance treatment: prescribed fire, managed wildfire, or mechanical fuels treatment. *Target range corresponds to 50-75% of dry open and 25-50% of moist open forests.*					

Figure 1.1 WADNR Forest health treatment summary table for Chumstick-LP. This table guided management implementation for project's simulation experiment.

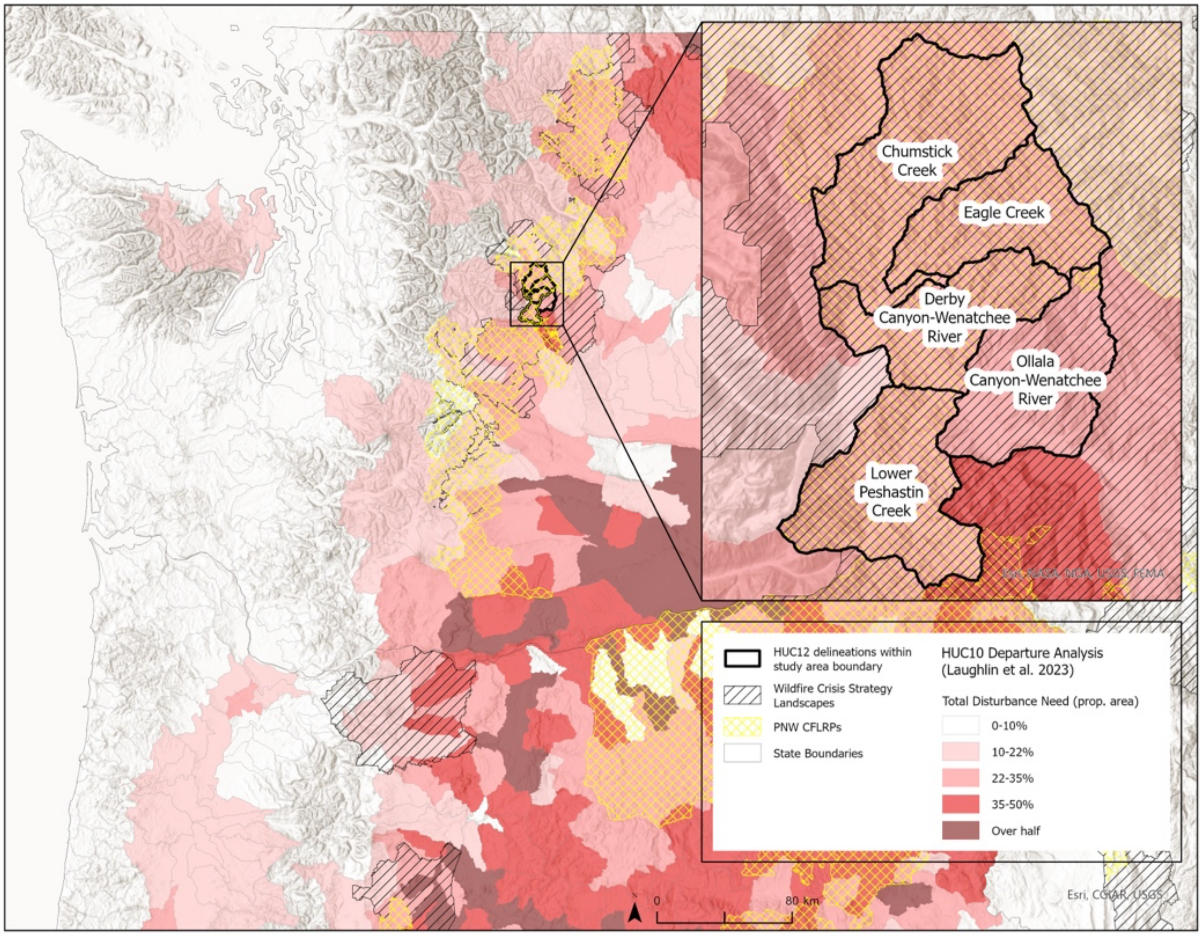

Figure 1.2 Study area overlaid with dedicated priority areas for management under USFS forest health initiatives, and with disturbance-only restoration need. Disturbance only indicates land that would become restored after treatment such as prescribed fire and/or thinning (Laughlin et al., 2023).

2.2 Model initialization

To initialize the focal landscape in iLand, spatially explicit topography, soil (texture, fertility, and depth), climate, and tree-level vegetation data were collected and prepared for input into iLand. Calibration of tree species, wildfire, and carbon parameters for the range of environmental conditions across the focal landscape was completed before an evaluation of landscape-level patterns of species composition and successional dynamics.

2.2.1 Initial grid and coordinate reference system

Spatially explicit gridded data were added to the modeled landscape by first defining an extent and coordinate system for downloading and preparing for input into iLand. Using a 31.7 by 61.2 km frame around the Chumstick-LP planning area, we first extracted the 10-meter resolution digital elevation model ("10-meter DEM files in the Wenatchee 1° by 2° quadrangle," n.d.) and projected the grid to Albers Equal Area Conic and the North American Datum of 1983 (ESPG: 4269) coordinate reference system. After this step, the DEM grid was resampled to 100m resolution to create a 'based grid' from which to extract all other input gridded datasets.

2.2.2 Climate model selection

To simulate a hot and dry future, we selected a downscaled CMIP5 global climate model with the 'worst-case' emissions scenario—HadGEM2-ES365 with representative concentration pathway (RCP) 8.5—from the Multivariate Adaptive Climate Analogs v2 (MACAv2) database (Abatzoglou and Brown, 2012) based on annual temperature and precipitation trends relative to the suite of global climate models for eastern Washington (Table 1.2). In eastern Washington, HadGEM2-ES365 RCP 8.5 predicts a steady increase in maximum summer and winter temperatures throughout the century, with the summer maximum temperature by 2099 nearly five degrees Fahrenheit above the median summer maximum across other CMIP5 RCP 8.5 models, and over ten degrees Fahrenheit above the summer maximum in the early part of the century. HadGEM2-ES365 predicts a dry future with the maximum number of consecutive days with daily precipitation below 0.2mm increasing to over 40 by mid-century, and annual total precipitation dropping 2.7in below the median across other CMIP5 RCP 8.5 models by 2099 ("Climate Toolbox," n.d.).

Table 1.2 Comparing HadGEM2-ES365 with representative concentration pathway 8.5 CMIP5 with median across models for eastern WA using the Climate Toolbox tool, which compares downscaled climate projections from the MACAv2 database.

	Jun-July-Aug Daily Max (ºC)		Dec-Jan-Feb Daily Min (ºC)		Annual Total Precipitation (cm)		Max consecutive dry days*	
Year	HadGEM2-ES365	Diff. from med	HadGEM2-ES365	Diff. from med	HadGEM2-ES365	Diff. from med	HadGEM2-ES365	Diff. from med
2010-2039	27.4	0.6	-3.7	-0.1	72.6	1.0	34.9	-0.2
2040-2069	30.2	1.2	-1.6	0.7	75.2	0.8	41.5	4.2
2070-2099	34.1	2.6	0.4	0.6	70.4	-6.9	43.8	3.2

*Precipitation below 0.2 mm

2.2.3 Environmental inputs

Gridded environmental inputs, including soil texture, fertility, and daily climate data, were used in the model at the resolution of resource units (RU), or 100x100m pixels. We extracted soil texture and soil depth inputs from the CONUS-SOIL dataset (Miller and White, 1998), which maps soil characteristics for the coterminous USA at a 1km resolution. We collected modeled daily climate data at 4km resolution for each RU for each climate scenarios from 1960 to 2100 from the MACAv2 database (Abatzoglou and Brown, 2012). These data were compiled into a SQLITE database for input into iLand. Available nitrogen data was configured from published datasets (Coops, 2015), in which a process-based model (3PG) was used to model soil fertility from MODIS remote sensing inputs. Each environmental variable was recorded in a text file within the project directory.

2.2.4 Vegetation inputs

We used the TreeMap2016 dataset to add a single initial vegetation layer that is constant across all scenarios (Riley et al., 2022). TreeMap uses Forest Inventory Assessment (Gray et al., 2012) plot data and LANDFIRE (Rollins, 2009) spatial data to spatially impute forest inventory data onto a wall-to-wall 30m grid across the continental United States based on LANDFIRE vegetation cover, forest type, disturbance history, and vegetation height data. Using this dataset, we assigned PNW-only tree lists to each 100m pixel across the model landscape. Since iLand uses each pixel's tree list to randomly place trees at the start of each new simulation, a 'snapshot' of the initial model landscape was taken to save the coordinates of each tree and create an identical vegetation layer for the start (i.e. calendar year 2025) of each simulation of this experiment.

2.2.5 Species calibration

Sixty-four demographic parameters for 20 major and minor PNW tree species were collected from previous iLand projects and datasets, including parameters for six new PNW subcanopy and resprouting deciduous tree species that were collected in 2021-2022 (Thom et al., 2024). All twenty-six species were calibrated for the extent of Washington and Oregon based on a pattern-oriented modeling approach (Grimm et al., 2005) to realistically represent patterns of complex forest dynamics driven by bottom-up processes like stress response, species competition, and successional dynamics. The original parameter geographic ranges and parameter data sources of all species that were calibrated for the PNW are listed in Table 1.3 (Kruszka et al., *In prep*). Species-specific light influence patterns were configured outside of iLand using the light influence pattern generator Lightroom, which takes height-diameter equations, crown height parameters and the average latitude of the simulation area as inputs (Seidl et al., 2012a). After calibration, iLand appropriately represented patterns of height and diameter growth, mortality and aging, and regeneration for each species. At the stand level, iLand appropriately represented patterns of competition and succession for forest types across the topo-climatic gradient of Washington and Oregon (Kruszka et al., *In prep*).

Table 1.3 Original geographic range and data source of each tree species calibrated for WA/OR.

Orig. geo. range	Orig. data source	Species	Common name
HJ Andrews Experimental Forest, OR	(Seidl et al., 2012a)	*Abies amabilis* (Douglas ex Loudon) Douglas ex Forbes	Pacific silver fir
		Abies grandis (Douglas ex D. Don) Lindl.	grand fir
		Abies procera Rehder	noble fir
		Acer macrophyllum Pursh	bigleaf maple
		Pinus ponderosa Lawson & C. Lawson	ponderosa pine
		Picea sitchensis (Bong.) Carrière	Sitka spruce
		Pseudotsuga menziesii (Mirb.) Franco var. *menziesii*	coastal Douglas-fir
		Thuja plicata Donn ex D. Don	western redcedar
		Tsuga heterophylla (Raf.) Sarg.	western hemlock
		Tsuga mertensiana (Bong.) Carrière	mountain hemlock
	(Seidl et al., 2012b)	*Alnus rubra* Bong.	red alder
Not previously used	(Kruszka et al., *In prep*; Thom et al., 2024)	*Callitropsis* nootkatensis (D. Don) Oerst. ex D.P. Little	Alaska yellow-cedar
		Chrysolepis chrysophylla (Douglas ex Hook.) Hjelmqvist	golden chinquapin
		Cornus nuttallii Audubon ex Torr. & A. Gray	Pacific dogwood
		Populus balsamifera L. ssp. *trichocarpa* (Torr. & A. Gray ex Hook.) Brayshaw	black cottonwood
		Prunus emarginata (Douglas ex Hook.) D. Dietr.	bitter cherry
		Taxus brevifolia Nutt.	Pacific yew
Not previously used	(Thom et al., 2024)	*Larix lyallii* Parl.	subalpine larch
		Larix occidentalis Nutt.	western larch
		Pinus monticola Douglas ex D. Don	western white pine
Greater Yellowstone Ecosystem	(Turner et al., 2022b)	*Pinus albicaulis* Engelm.	whitebark pine
		Populus tremuloides Michx.	quaking aspen
	(Braziunas et al., 2018); (Hansen et al., 2018)	*Abies lasiocarpa* (Hook.) Nutt.	subalpine fir
		Pinus contorta Douglas ex. Loudon var. latifolia Engelm. ex S. Watson	lodgepole pine
		Picea engelmannii Parry ex Engelm.	Engelmann spruce
		Pseudotsuga menziesii (Mirb.) Franco var. *glauca* (Beissn.) Franco	Rocky Mountain Douglas-fir

2.2.6 Wildfire module calibration

To calibrate the dynamic wildfire module in iLand to resemble the contemporary wildfire regimes in interior forests of the PNW, we followed the approach of (Seidl et al., 2014) to adjust fire module parameters based on comparisons of simulated mean fire return interval, wildfire size distributions, shape, and severity with a reference dataset. Model outputs were generated from simulations of the focal landscape with wildfire disturbance for 100-300 years, starting with default parameters, then with iterative adjustments after comparative analysis with reference data (Appendix A.3). To compare simulated mean fire return interval, fire size, and fire shape with the target wildfire record, we used a CONUS-wide reference dataset of wildfire perimeters that date from 1835-2020 (Welty and Jeffries, 2021). When cropped to forested areas of eastern Washington and Oregon, 2,935 fires remained in the dataset, with the oldest fire on record being in 1885. We did not focus on one specific fire regime group and instead included the entire range of wildfire frequency and severity patterns east of the Cascade Crest in Washington and Oregon.

To compare wildfire severity with the target wildfire record, we used wildfire perimeter and severity data from the Monitoring Trends in Burn Severity (Eidenshink et al., 2007) dataset within the spatial extent of eastern Washington and Oregon, which included 612 wildfires dating from 1987 to 2024. Successful calibration was determined by how closely each wildfire regime characteristic (mean fire return interval, wildfire size distributions, shape, and severity) matched the range of wildfires in the reference datasets. See Appendix table A.3.3 for the default and final calibrated wildfire module parameters.

2.2.7 Carbon calibration

We calibrated dynamic carbon cycling—rates of carbon movement across above- and below-ground live trees, snags, downed woody debris (downed logs and large branches), the forest floor (litter and small branches), and soil—in iLand (Appendix A.4) for eastern Washington and Oregon. Over 240 1-ha FIA plots spanning the topo-climatic gradient of eastern Washington and Oregon were initialized in iLand and run for 500 years. Output carbon stocks (Mg/ha) were compared to reference datasets for eastern Washington and Oregon forest types (i.e., A. Gray et al., 2016; A. Gray and Whittier, 2014; Smithwick et al., 2002; Raymond and McKenzie, 2013) to guide adjustments of species-specific parameters ruling decomposition rates

(Appendix table A.4.3). Successful calibration of carbon dynamics was determined by how closely each simulated carbon pool at equilibrium matched reference carbon pools (Mg/ha). See Appendix tables A.4.3 and A.4.4 for calibrated species-specific carbon parameters and default carbon constants, respectively.

2.2.8 Landscape evaluation

To evaluate the Chumstick-LP landscape and observe how modeled patterns of successional dynamics and species composition across the topo-climatic gradient match expected patterns across space and time (Seidl et al., 2012), we initialized the full model landscape in iLand with calibrated species, wildfire, and carbon parameters. We ran the landscape with and without fire for a period of 500 years and compared species-specific and total basal area (m^2/ha) across elevation and time. Successful evaluation was determined by how well species composition, stand-level basal area, stand-level density, and carbon pools matched expectations for the elevational gradient. See Appendix A.5 for landscape evaluation results.

2.3 Deterministic management plan

To implement a spatially explicit management plan that addresses anticipated treatment need, we assigned each 100m pixel of the model landscape to one of three fuel reduction treatments based on the initial vegetation layer. Assignment of each treatment category—commercial thin from below with surface fuel reduction, noncommercial thin with surface fuel reduction, maintenance surface fuel reduction—was guided by the WADNR Forest Health Summary Table for the focal landscape (Figure 1.1) ("20-Year Forest Health Strategic Plan: Eastern Washington | Department of Natural Resources," n.d.). For example, Medium-Large dense dry forests were assigned a commercial thin treatment due to overrepresentation of closed canopy forests and an underrepresentation of open canopy forests. The Forest Health Summary Table uses forest structure (defined by the 6-box structure class scheme, Table 1.1, which closely aligns with the 5-box structure class scheme) and dry/moist forest type classifications to assign a treatment, thus we assigned treatments to pixels using the same 6-box forest structure classification scheme as the Forest Health Summary Table (WADNR, 2020) and forest type (Rollins, 2009). We took note of dominant species cover for each pixel to identify a generic stand density index using the Okanogan-Wenatchee National Forest Field Guide (Lillybridge et al., 1995), which lists stand density indices by dominant overstory species and understory plant associations. Commercial thin treatments were assigned a target density equal to 35% of the stand density index based on dominant species cover. Operational filters—inventoried roadless, wilderness areas, private land, and late seral reserves—were used to restrict management to where it would most likely occur. In total, 5,255 ha were assigned commercial thinning from below with surface fuel removal, 5,204 ha were assigned noncommercial thinning with surface fuel removal, and 1,613 ha were assigned maintenance surface fuel reduction.

The details and mechanics of each of the three categories of treatment were coded in JavaScript (Table 1.4) and paired with the management map (Table 1.5 and Figure 1.3). In each future scenario with management enabled, each pixel was managed at a 20-year rotation, an appropriate rotation for the modeled treatment intensities in eastern WA forests (Radcliffe et al., 2024), and 1/5 of the landscape was treated every four years. To evaluate whether the landscape-scale management schedule (i.e., 1/5 of the landscape every four years) influenced the FRV, we conducted a sensitivity analysis with four different management schedules (1/2 of the landscape treated every ten years, 1/4 every five, 1/5 every four, 1/20 every year). We found that the management schedule did not influence the FRV (Appendix A.6).

Table 1.4 Treatments used in deterministic management plan, descriptions of how they were implemented each in iLand

Treatment	Step #	Protocol	Description*
Commercial thin + fuels treatment	1	Kill saplings	Remove all trees with height below 4 m
	2	Thin from below then pile burn (skip if density is below target density)	Find target trees/ha using dominant species and Wenatchee NF Field Guide Appendix G. Remove trees in bottom 50% of DBH, then remove remaining trees from upper percentile to reach the target trees/ha. From the harvested trees: remove 80% of the foliage/branch biomass, 100% of stems.
	3	Remove surface fuels (regardless of stand density)	Remove 50% of DWD, 85% of litter, 10% of SOM
Non-commercial thin	1	Kill saplings	Remove all trees with height below 4 m
	2	Remove all trees below 8in DBH then pile burn	From harvested trees: remove 80% of foliage/branch biomass, 100% of stems
	3	Remove surface fuels	Remove 50% of DWD, 85% of litter, 10% of SOM
Maintenance fuel reduction	1	Kill saplings	Remove all trees with height below 4 m
	2	Remove surface fuels	Remove 50% of DWD, 85% of litter, 10% of SOM

*SOM = soil organic matter, DWD = downed woody debris, DBH = diameter at breast height
.

Table 1.5 Codes assigned to each pixel available for management correspond to a treatment type and a treatment schedule. See Figure 1.3 for a map of the treatment codes. Com. = commercial, Noncom. = noncommercial.

Code	Treatment type	First year of treatment
1	Com. Thin	1
2	Noncom. Thin	1
3	Maintenance	1
11	Com. Thin	5
12	Noncom. Thin	5
13	Maintenance	5
21	Com. Thin	10
22	Noncom. Thin	10
23	Maintenance	10
31	Com. Thin	15
32	Noncom. Thin	15
33	Maintenance	15
41	Com. Thin	20
42	Noncom. Thin	20
43	Maintenance	20

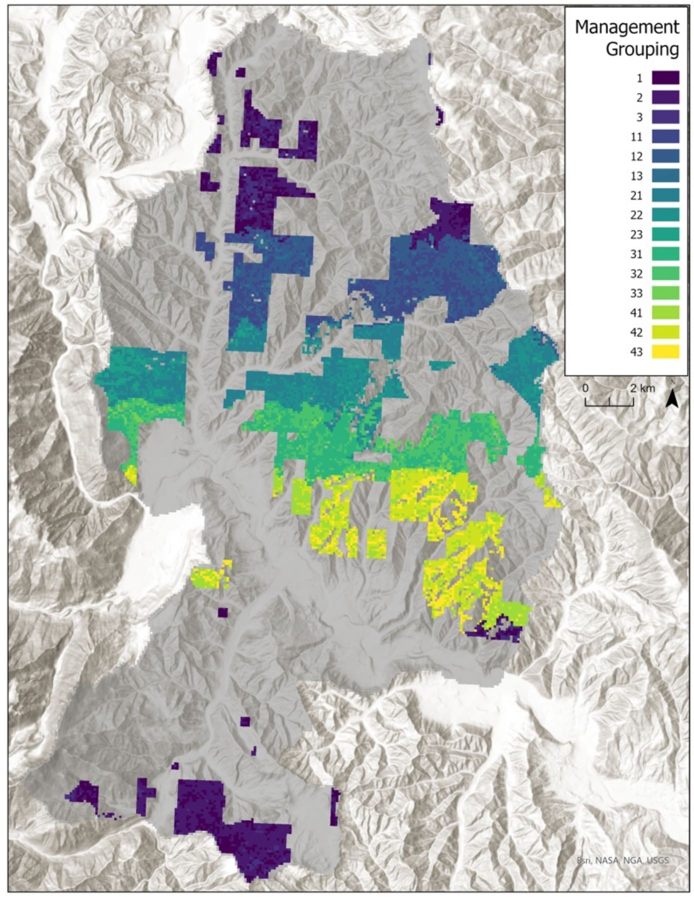

Figure 1.3 Map of deterministic management plan. Each color corresponds to the codes defined in Table 1.5

2.4 Simulation design

Ten trials of 75-year simulations were run for each of eight different scenarios combining different major drivers of change (i.e., fire, management, and climate change) in a 2 X 2 X 2 factorial experiment in which each driver of change is enabled or disabled (total number of simulation trials = 80. See Table 1.6). In trials with climate change disabled, climate years were randomly sampled from the first thirty years of the selected HadGEM2-ES365 RCP 8.5 climate dataset (1950-1980) with replacement. In trials with climate change enabled, climate years began at 2025 and continued sequentially until 2099. Vegetation and soil inputs remained constant for all scenarios (listed in Table 1.6). A scenario with all drivers of change (fire, climate change, management) disabled was run to demonstrate forest change due to succession and compare with other scenarios.

Table 1.6 Summary of experimental design: a 2 X 2 X 2 factorial framework (10 trials, 80 total simulations). F = Fire, M = Management, C = Climate change. 'X' = enabled, '–' = disabled.

Scenario number	Name	Fire	Climate change	Management
1	F	X	–	–
2	M	–	–	X
3	C	–	X	–
4	FCM	X	X	X
5	FC	X	X	–
6	FM	X	–	X
7	CM	–	X	X
8	N	–	–	–

2.5 Data analysis

2.5.1 Dividing the landscape into forest types

The selected rRV is from the Haugo et al. (2015) dataset, which used the 5-box structure classification (i.e., early, mid-seral closed canopy, mid-seral open canopy, late-seral open canopy, late-seral closed canopy) (Figure 1.1), is specific to LANDFIRE biophysical settings, or forest types. To specify the FRV of each scenario to forest types in the landscape, and for more direct comparison with the rRV estimates from Haugo et al. (2015), the full landscape was masked to the three most abundant forest types. The three most abundant forest types (in order of most to least abundant) were Mixed Conifer – Eastside Dry making up 51.7 % (from here on called ‘dry’), Mixed Conifer – Eastside Mesic making up 23.4% (from here on called ‘moist), and Dry Ponderosa Pine – Mesic making up 22% (from here on called ‘pipo’). See Figure 1.4 and Appendix table A.2 for details on the forest type composition across the Chumstick-LP planning area.

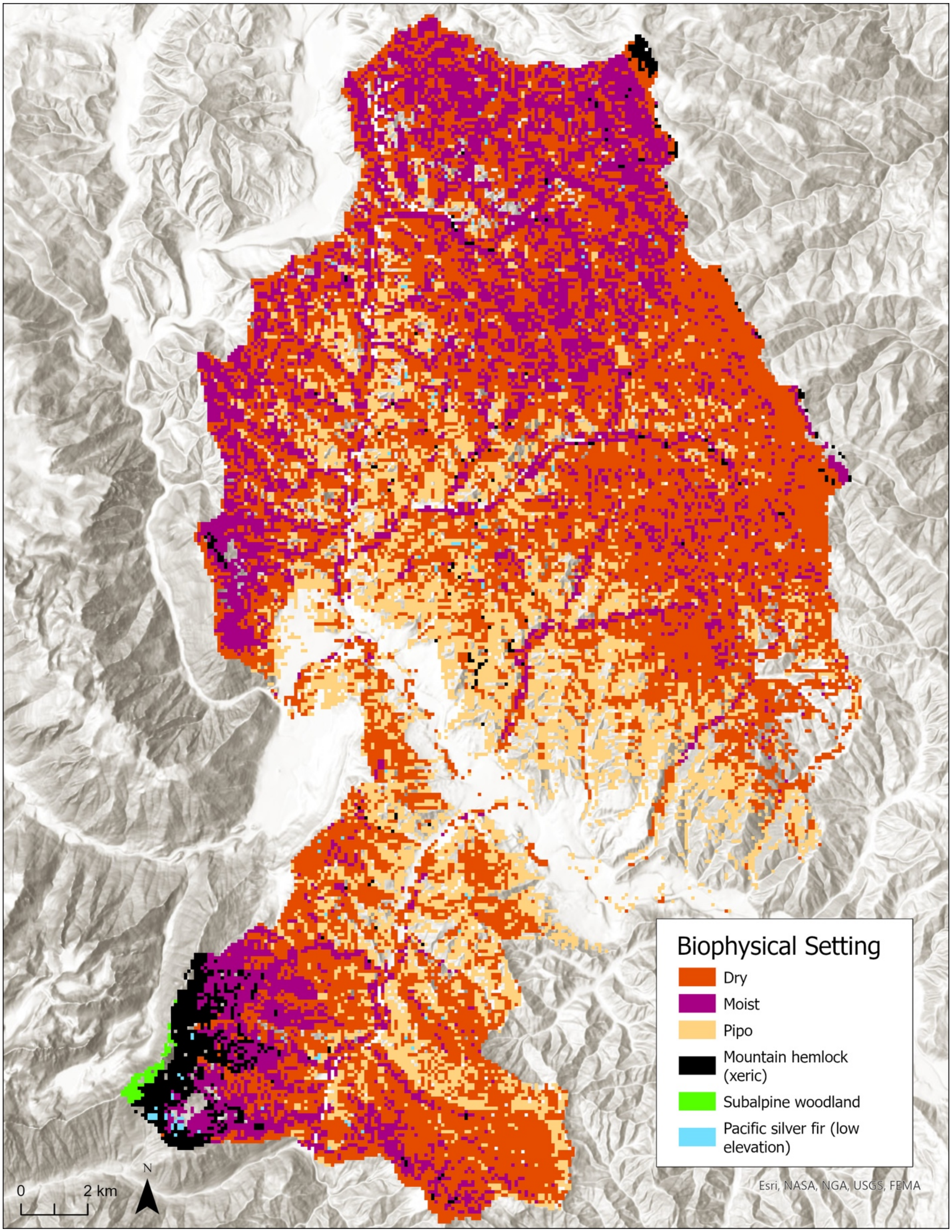

Figure 1.4 Map of LANDFIRE biophysical settings across focal landscape. 'Pipo' stands for ponderosa pine forest.

2.5.2 Creating annual structure class rasters from iLand outputs

To classify a raster of structure classes from simulation outputs to estimate and directly compare the FRV of structure class composition with the rRV from Haugo et al. (2015), we followed the 5-box structure class model, which was used by Haugo et al. (2015) (Figure 1.1).

Annual outputs of the 85th percentile diameter and percent canopy cover for each 1 ha pixel were used to create annual structure class rasters that match the 5-box classification of Haugo et al. (2015) (Table 1.1). However, to account for the difference between typical tree inventory datasets, which may exclude trees below a 5 in. or 10 cm size class, and iLand tree outputs, which include all trees above 4 m height, the diameter threshold between early and mid-seral classes was adjusted from 25.4 cm to 12.7 cm diameter. Additionally, to avoid confounding post-fire, early seral forest with mid-seral forest where shade-tolerant stems create a dense understory that bring the 85th percentile diameter below 12.7 cm, forests with an 85th percentile diameter below 12.7 cm and canopy cover greater than 10% were assigned as mid-seral. To stay consistent with the crucial threshold determining mid-seral from late-seral, which has implications for management restriction policies in a stand, the 50.8 cm diameter threshold between mid-seral and late-seral remained the same (Table 1.7).

Table 1.7 Original (WADNR, 2020) and adjusted 5-box structure class definitions. Adjustments were made to account for the difference between typical tree inventory datasets that leave out the smallest size classes, and iLand tree outputs, which include all trees.

Structure class	5-box model original definition*	Adjusted definition
Early	CACO < 10% | DBH < 25.4 cm, CACO >= 10% AND <40%	DBH < 12.7 cm, CACO <= 10%
Mid-Open	DBH >= 25.4 cm AND < 50.8 cm, CACO >= 10% AND < 40%	DBH >= 12.7 cm AND < 50.8 cm, CACO >= 10% AND < 40%
Mid-Closed	DBH >= 25.4 cm AND < 50.8 cm, CACO >= 40%	DBH >= 12.7 cm AND < 50.8 cm, CACO >= 40%
Late-Open	DBH >= 50.8 cm, CACO >= 10% AND < 40%	DBH >= 50.8 cm, CACO >= 10% AND < 40%
Late-Closed	DBH >= 50.8 cm, CACO >= 40%	DBH >= 50.8 cm, CACO >= 40%

*CACO = canopy cover, DBH = quadratic mean diameter of largest 25% trees

To assess how the original and adjusted structure class definitions influenced structure class transitions due to management in iLand, we compared the structure class distributions one year pre- and post-management between original and adjusted. Results (see Appendix A.7) show that original definitions yield unexpected transitions of structure classes pre- and post-management (early seral forest should not jump to mid-seral open or closed canopy forest after management, or within the span of one year). Adjusted definitions yield expected structure class distributions both pre- and post-management (mid-seral closed should transition to mid-seral open when treated for density or fuel reduction, mid-seral open canopy should stay the same. No early seral because there is no wildfire disturbance yet). Output structure class rasters were saved at the full extent of the model landscape, for dry mixed conifer forests only, for moist mixed conifer forests only, and for mesic ponderosa pine forests only.

2.5.3 Calculation of landscape metrics

To quantify the composition and pattern of forest structure over time for each scenario, percent land, patch density, and arithmetic mean patch size of each structure class were calculated for each year of each trial using the Landscape Metrics ('landscapemetrics') package in R (Hesselbarth et al., 2019). These metrics were calculated for the full landscape, dry mixed conifer, moist mixed conifer, and ponderosa pine forests. The arithmetic mean patch size (as opposed to the weighted mean patch size) was chosen to match metrics used in other rRV estimates for the region (i.e., Hessburg et al., 1999). These metrics were selected because they characterize the composition (i.e., percent cover and mean patch size) and pattern or continuity (i.e., patch density) of structure classes across a given landscape (Hessburg et al., 1999). Although percent cover directly informs how much land is covered by a certain structure class, mean patch size provides information on whether the percent cover is in large or small patches, and patch density further shows whether the class cover is fragmented (high patch density) or more continuous (low patch density).

2.5.4 Assessing future trends of structure class composition and pattern across scenarios

To estimate the FRV of landscape-level structure class composition (percent land) and pattern (patch density, mean patch size) for each scenario, we summarized each landscape metric from each year between year 2025 and 2099 across trials for each forest type setting (n = 750).

2.5.5 Comparing structure class composition FRV and rRV across scenarios

The Haugo et al. (2015) dataset presents the rRV as the mean ± 2 standard deviations percent land for each forest type (Table 1.8), derived from ten simulations of 500 annual time-steps (n = 5000) for each forest type. For a 1:1 comparison of the FRV of structure class composition (percent land) of each scenario with the Haugo et al. (2015) rRV, the mean and range of ± 2 standard deviations of structure class categories (n = 750) were compared to the Haugo et al. (2015) rRV estimates for each forest type.

Table 1.8 Haugo et al. (2015) reference range of variability of structure class composition for the three most abundant biophysical (BpS) settings, labeled according to LANDFIRE. Each BpS setting has a characteristic fire regime group (FRG) and corresponding landscape unit level (LL). Reference conditions for dry and pipo forests, which historically burned frequently by low severity fire, were assessed at the smallest landscape level (LL = 1, or ~46,000ha), while reference conditions for moist forests, which historically burned between 35 and 200 years by mixed low to moderate severity fire, were assessed at one level greater (LL = 2, or ~285,000ha).

BpS	short name	Sclass	Mean	Mean – 2SD	Mean + 2SD	FRG	LL*
Mixed conifer—dry	*(dry)*	Early	14.0	11.7	16.3	1	1
		Mid-Closed	0.66	0.18	1.13	1	1
		Mid-Open	31.6	28.8	34.5	1	1
		Late-Open	41.5	38.2	44.7	1	1
		Late-Closed	12.3	10.3	14.4	1	1
Mixed conifer—moist	*(moist)*	Early	14.5	12.4	16.6	3	2
		Mid-Closed	44.4	41.5	47.3	3	2
		Mid-Open	12.5	10.4	14.6	3	2
		Late-Open	9.64	7.79	11.5	3	2
		Late-Closed	18.9	16.7	21.2	3	2
Ponderosa pine—mesic	*(pipo)*	Early	10.8	8.91	12.6	1	1
		Mid-Closed	6.89	5.46	8.33	1	1
		Mid-Open	37.2	34.3	40.1	1	1
		Late-Open	42.4	39.2	45.5	1	1
		Late-Closed	2.77	1.71	3.83	1	1

3. Results

3.1 Effects of fire, future climate change, and management on the future range of variability of structure class composition and pattern

Overall, fire, climate change, and management each affected landscape-scale structure class composition and pattern, but wildfire qualitatively drove more change than climate change and management (expected, in line with findings from Churchill et al., 2022 and Laughlin et al., 2023). Here, we compare results for the most ecologically meaningful and realistic scenarios: no wildfire, climate change, or management (null, N), wildfire only (F), climate change only (C), wildfire and climate change (FC), and wildfire, climate change, and management (FCM).

Across all scenarios, average structure class percent land across the entire 75-year simulation ranged from 0-3.8% early seral, 29.8-63% mid-seral closed canopy, 28.9-38.6% mid-seral open canopy, 3.8-33.1% late-seral open canopy, and 0.9-4.8% late-seral closed canopy (See Table 1.9 for percent land FRVs). Average structure class mean patch size (mean patch size in a single given year) ranged from 1.2-2.9 ha early seral, 27.1-60 ha mid-seral closed canopy, 10.6-14.8 ha mid-seral open canopy, 1.8-20.9 ha late-seral open canopy, and 1.4-2.2 ha late-seral closed canopy (see Table 1.10 for mean patch size FRVs). Average structure class patch density ranged from 3.2-118.1 patches/10,000 ha early seral, 80.5-208.6 patches/10,000 ha mid-seral closed canopy, 269.1-322.4 patches/10,000 ha mid-seral open canopy, 167.5-260.4 patches/10,000 ha late-seral closed canopy, and 61.8-198 patches/10,000 ha late-seral open canopy (See Table 1.11 for patch density FRVs).

Wildfire reduced the percent cover, mean patch size, and patch density of mid-seral closed-canopy forest while increasing the percent cover and continuity of late seral, open canopy forests (when compared to the null). Compared to the null scenario, F scenario had a lower average area and mean patch size of mid-seral closed canopy forests (mid-closed)—by a difference of 23.4% and 16ha—and a higher average percent land and mean patch size of late-seral open canopy forest (late-open)—by a difference of 25.9% and 14.8 ha, respectively. The F scenario also reduced the patch density of mid-seral closed canopy and late-seral open canopy and forest by 52.7 and 33 patches per 10,000 ha, respectively. The addition of wildfire increased the average percent land, mean patch size, and patch density of early seral forest by a difference of 3.8%, 1.7 ha, and 114.9 patches per 10,000 ha, respectively. In the climate change (C) scenario, the mean percent land of mid-seral closed canopy forest increased by a difference of 2.5% and mean percent land of late-seral closed canopy forest (late-closed) increased by 2.1% compared to the null model. When wildfire and climate change were both turned 'on' in iLand (FC), the average percent land covered by late-seral open canopy forest decreased—by a difference of 2.7%—and the average percent land covered by mid-seral closed canopy forest increased—by a difference of 6.3%—compared to the fire-only scenario. The addition of management to the fire and climate change scenario (FCM) reduced the average percent land and mean patch size of mid-seral closed canopy forest by 4.8% and 17.3 ha, respectively, when compared to fire and climate change without management, or the FC scenario. Additionally, when compared to the FC scenario, the patch density of mid-seral closed canopy forest in FCM increased from 80.5 to 111.3 patches per 10,000 ha, or a difference of 30.8. Comparing late-seral open canopy between FCM and FC scenarios, mean percent land was higher by 4.6%, mean patch size was higher by 2.6 ha, and patch density was lower by 0.5 patches per 10,000 ha with the addition of management.

3.2 Comparing FRV of structure class composition and rRV – dry forests

Wildfire and management reduced the mean percent land covered by mid-seral closed canopy structure in mixed conifer dry forests but did not bring the mean into the rRV range. In F scenario, mid-seral closed canopy mean and range percent land (0-78.2%) exceeded the rRV mean of 0.66% by a difference of 29.2% and overlapped the rRV range. In C scenario, mid-seral closed canopy mean and range percent land (39-91%) exceeded the rRV mean by a difference of 64.3% and exceeded (did not overlap) the rRV range. In FC scenario, mid-seral closed canopy mean and range percent land (0-72%) exceeded the rRV mean by a difference of 35.4 and overlapped the rRV range. In FCM scenario, mid-seral closed canopy mean and range percent land (0-78%) exceeded the rRV mean by a difference of 35.4% and overlapped the rRV range. See Table 1.12 for all FRVs.

Mean percent cover of late seral forest covered less area across all FRV scenarios compared to the rRV in dry forests. In F scenario, late-seral open canopy mean percent land was less than the rRV by a difference of 10.7%. In C scenario, late-seral open canopy mean percent land was less than the rRV mean by a difference of 38%, and the range partially overlapped with the rRV range. In FC scenario, late-seral open canopy mean percent land was less than the rRV mean by a difference of 12.7%. In FCM scenario, late-seral open canopy mean percent land was less than the rRV mean by a difference of 12.7%. See Figure 1.5 for dry forest FRV comparisons, and Table 1.12 for FRVs of all forest types across five scenarios.

3.3 Comparing FRV of structure class composition and rRV – moist forests

Mean percent cover of open canopy forests far exceeded the rRV range in moist mixed conifer forests across all scenarios. In F scenario, mid-seral open-canopy percent land was greater than the rRV mean by a difference of 22.3% and overlapped the rRV range (10.4-14.6%). In C scenario, mid-seral open canopy mean percent land of 26% was greater than the rRV by a difference of 13.4% and overlapped with the rRV range. In FC scenario, mid-seral open canopy mean percent land of 32% was greater than the rRV by a difference of 17.4%, and the range overlapped with the rRV range. In FCM scenario, mid-seral open canopy mean percent land of 32% was greater than the rRV by a difference of 17.4%, and the range exceeded that of the rRV. See Figure 1.6 for moist FRV comparisons, and Table 1.12 for FRVs of all forest types across five scenarios.

3.4 Comparing FRV of structure class composition and rRV – pipo forests

Similar to dry forests, wildfire and management reduce the mean percent land covered by mid-seral closed canopy structure in ponderosa pine forests, but do not bring the mean into the rRV range. In F scenario, mid-seral closed canopy mean percent land (0-73.3%) was greater than the rRV mean of 6.89% by a difference of 20%. In C scenario, mid-seral closed canopy mean percent land (31-89%) exceeded the rRV mean by a difference of 53.3% and the range completely exceeded the rRV range. In FC scenario, mid-seral closed canopy mean percent land (0-74.6%) was greater than the rRV mean by a difference of 26.7%. In FCM scenario, mid-seral closed canopy mean percent land (70.6%) exceeded the rRV mean by a difference of 21.7%. See Figure 1.7 for pipo FRV comparisons, and Table 1.12 for FRVs of all forest types across five scenarios.

Table 1.9 Min, max, median, mean, sd of percent land of structure classes from 2025-2099 for ten trials (n=750) of eight scenarios. F = Fire, M = Management, C = Climate change.

Scenario	Struct. class	min	max	median	mean	sd
F	Early	0.0	13.7	3.7	3.8	2.7
	Mid-Closed	2.7	84.7	20.0	29.8	23.5
	Mid-Open	14.0	57.4	34.3	34.3	10.1
	Late-Open	0.4	64.2	32.9	31.2	16.0
	Late-Closed	0.2	2.5	0.9	0.9	0.5
M	Early	0.0	0.3	0.1	0.1	0.1
	Mid-Closed	23.8	84.7	42.1	45.9	17.1
	Mid-Open	14.0	45.7	43.0	38.6	8.8
	Late-Open	0.4	26.6	11.6	12.5	7.9
	Late-Closed	0.9	4.3	3.2	2.9	1.2
C	Early	0.0	0.1	0.0	0.0	0.0
	Mid-Closed	35.8	84.4	64.3	63.0	13.4
	Mid-Open	14.1	38.5	30.3	28.9	7.3
	Late-Open	0.4	12.4	2.3	3.8	2.9
	Late-Closed	0.9	13.9	2.0	4.3	3.8
FCM	Early	0.0	7.1	2.0	2.0	1.3
	Mid-Closed	4.4	84.4	23.1	31.3	21.0
	Mid-Open	14.1	46.8	32.5	31.7	6.2
	Late-Open	0.4	74.1	35.7	33.1	18.1
	Late-Closed	0.6	4.6	1.5	1.8	0.9
FC	Early	0.0	12.4	2.4	2.8	2.2
	Mid-Closed	3.7	84.4	29.4	36.1	20.8
	Mid-Open	14.1	52.4	31.3	31.3	8.2
	Late-Open	0.4	71.7	29.2	28.5	15.7
	Late-Closed	0.3	5.2	1.0	1.4	1.0
FM	Early	0.0	10.5	2.0	2.2	1.7
	Mid-Closed	4.9	84.6	23.2	30.9	20.9
	Mid-Open	14.0	54.0	36.7	36.9	8.5
	Late-Open	0.4	58.4	29.6	28.5	14.6
	Late-Closed	0.6	3.6	1.4	1.6	0.6
CM	Early	0.0	0.3	0.1	0.1	0.1
	Mid-Closed	25.9	84.5	46.4	49.0	15.8
	Mid-Open	14.1	41.8	37.5	35.0	6.8
	Late-Open	0.4	25.1	9.2	11.1	7.3
	Late-Closed	0.9	10.8	3.7	4.8	3.2
N	Early	0.0	0.1	0.0	0.0	0.0
	Mid-Closed	39.5	84.6	59.3	60.4	13.3
	Mid-Open	14.1	43.7	34.3	32.1	9.1
	Late-Open	0.4	13.1	4.4	5.3	3.5
	Late-Closed	0.9	3.9	2.0	2.2	0.9

Table 1.10 Min, max, median, mean, sd of mean patch size (ha) of structure classes from 2025-2099 for ten trials (n=750) of eight scenarios. F = Fire, M = Management, C = Climate change.

Scenario	Struct. class	min	max	median	mean	sd
F	Early	1.0	7.2	2.9	2.9	1.1
	Mid-Closed	6.1	188.0	21.7	37.8	38.5
	Mid-Open	3.9	34.7	10.2	11.3	5.4
	Late-Open	1.1	49.3	15.0	17.0	10.4
	Late-Closed	1.1	2.1	1.4	1.4	0.2
M	Early	1.0	2.0	1.2	1.2	0.2
	Mid-Closed	9.8	187.7	16.8	31.9	35.6
	Mid-Open	3.9	18.5	16.6	14.8	4.0
	Late-Open	1.1	9.2	3.8	4.3	2.2
	Late-Closed	1.2	2.1	1.8	1.7	0.3
C	Early	1.0	2.0	1.2	1.2	0.2
	Mid-Closed	13.6	186.4	50.0	60.0	39.3
	Mid-Open	4.0	16.4	12.0	11.1	3.6
	Late-Open	1.1	3.6	1.6	1.8	0.5
	Late-Closed	1.3	5.2	1.4	2.1	1.0
FCM	Early	1.0	9.6	2.1	2.4	1.1
	Mid-Closed	5.2	188.4	19.3	32.1	33.5
	Mid-Open	4.0	19.6	10.5	10.6	2.8
	Late-Open	1.1	91.5	17.6	20.9	14.6
	Late-Closed	1.2	3.3	1.7	1.8	0.5
FC	Early	1.0	4.6	2.2	2.3	0.7
	Mid-Closed	10.2	186.3	34.8	49.4	38.5
	Mid-Open	4.0	27.6	10.6	11.0	4.5
	Late-Open	1.1	74.8	15.3	18.0	13.1
	Late-Closed	1.1	5.9	1.4	1.7	0.7
6	Early	1.0	7.6	2.4	2.6	1.0
	Mid-Closed	4.5	190.9	13.6	27.1	33.3
	Mid-Open	3.9	27.0	12.2	12.8	4.7
	Late-Open	1.1	38.4	11.8	13.2	7.4
	Late-Closed	1.2	2.2	1.5	1.5	0.2
7	Early	1.0	2.0	1.2	1.2	0.2
	Mid-Closed	9.6	186.2	21.2	35.1	35.7
	Mid-Open	4.0	17.4	14.0	13.0	3.1
	Late-Open	1.1	9.1	3.7	4.4	2.3
	Late-Closed	1.2	3.9	1.9	2.2	0.8
N	Early	1.0	2.0	1.1	1.2	0.2
	Mid-Closed	19.3	186.8	37.9	53.8	37.8
	Mid-Open	3.9	18.6	13.7	12.3	4.4
	Late-Open	1.1	4.0	1.9	2.2	0.7
	Late-Closed	1.3	2.2	1.5	1.6	0.2

Table 1.11 Min, max, median, mean, sd of patch density (Number per 10,000 ha) of structure classes from 2025-2099 for ten trials (n=750) of eight scenarios. F = Fire, M = Management, C = Climate change.

Scenario	Struct. class	min	max	median	mean	sd
F	Early	0.2	277.5	123.3	118.1	73.2
	Mid-Closed	43.9	153.1	84.6	88.9	25.6
	Mid-Open	165.5	426.3	328.7	322.4	50.2
	Late-Open	35.3	331.5	192.2	189.8	63.0
	Late-Closed	18.6	135.1	61.2	61.8	27.6
M	Early	0.2	22.2	9.2	8.5	6.3
	Mid-Closed	45.1	266.4	243.0	208.6	62.9
	Mid-Open	224.0	367.1	259.6	269.1	29.8
	Late-Open	34.3	330.1	297.8	260.4	75.7
	Late-Closed	63.5	221.6	180.4	161.2	46.3
C	Early	0.2	8.5	3.0	3.3	2.0
	Mid-Closed	45.3	265.2	130.1	136.4	54.3
	Mid-Open	230.7	356.7	256.6	271.6	34.8
	Late-Open	33.4	367.9	152.0	191.0	90.2
	Late-Closed	63.2	295.3	138.5	173.4	82.4
FCM	Early	0.2	200.6	93.0	87.0	49.9
	Mid-Closed	44.8	190.7	111.5	111.3	28.7
	Mid-Open	223.6	391.2	307.3	307.1	33.6
	Late-Open	34.6	275.4	169.9	167.5	46.1
	Late-Closed	47.1	178.5	85.7	94.1	31.8
FC	Early	0.2	375.5	108.0	108.1	68.4
	Mid-Closed	36.3	154.8	76.8	80.5	20.8
	Mid-Open	184.7	445.2	303.5	301.6	51.5
	Late-Open	33.9	311.8	171.7	168.0	59.2
	Late-Closed	26.1	154.3	69.6	73.0	28.8
FM	Early	0.2	194.9	80.4	78.6	46.8
	Mid-Closed	44.3	225.4	153.5	148.0	40.9
	Mid-Open	198.0	435.9	305.8	303.8	46.2
	Late-Open	34.8	309.6	225.3	215.1	56.3
	Late-Closed	45.0	182.1	97.0	98.6	29.0
CM	Early	0.2	22.9	10.7	9.5	6.9
	Mid-Closed	45.3	273.5	216.6	192.9	57.3
	Mid-Open	234.7	357.9	270.2	274.3	26.5
	Late-Open	34.3	296.6	251.6	229.6	63.7
	Late-Closed	63.7	313.8	198.5	198.0	78.9
N	Early	0.2	7.2	3.2	3.2	1.8
	Mid-Closed	45.3	205.9	155.4	141.6	44.0
	Mid-Open	231.2	364.4	254.8	271.3	34.5
	Late-Open	33.9	342.6	229.2	222.8	85.9
	Late-Closed	64.5	198.8	130.9	132.9	40.1

Table 1.12 Future range of variability (mean ± 2 standard deviation) for simulation period 2025-2099 across ten trials of five different fire (F), climate change (C), and management (M) scenarios in the three most common forest types in the focal landscape.

		N			F			C			FC			FCM		
BpS	Structure class	μ	μ – 2σ	μ + 2σ	μ	μ – 2σ	μ + 2σ	μ	μ – 2σ	μ + 2σ	μ	μ – 2σ	μ + 2σ	μ	μ – 2σ	μ + 2σ
Dry																
	Early	<1	0	<1	5	0	11	<1	0	<1	2	0	5	3	0	8
	Mid-Closed	64	40	89	30	0	79	65	39	91	30	0	73	36	0	80
	Mid-Open	30	12	47	34	11	57	28	13	43	32	18	45	31	13	49
	Late-Open	4	0	10	31	0	63	3	0	8	35	0	72	29	0	61
	Late-Closed	2	<1	4	1	0	2	4	0	12	2	0	3	1	0	3
Moist																
	Early	<1	<1	<1	5	0	11	<1	<1	<1	3	0	6	3	0	9
	Mid-Closed	63	35	91	33	0	85	68	42	93	36	0	82	39	0	85
	Mid-Open	31	11	51	35	10	59	26	11	41	32	15	49	30	11	48
	Late-Open	4	0	11	27	0	60	3	0	9	28	0	63	27	0	62
	Late-Closed	2	0	4	1	0	2	3	0	10	1	0	3	1	0	3
Pipo																
	Early	<1	<1	<1	3	0	7	<1	0	<1	2	0	4	2	0	6
	Mid-Closed	58	29	86	27	0	73	60	32	89	29	0	71	34	0	75
	Mid-Open	33	13	52	30	14	46	30	14	46	30	17	42	31	13	48
	Late-Open	7	0	15	39	1	77	5	0	11	38	0	78	32	0	65
	Late-Closed	3	1	4	1	0	2	5	0	13	2	<1	4	2	0	4

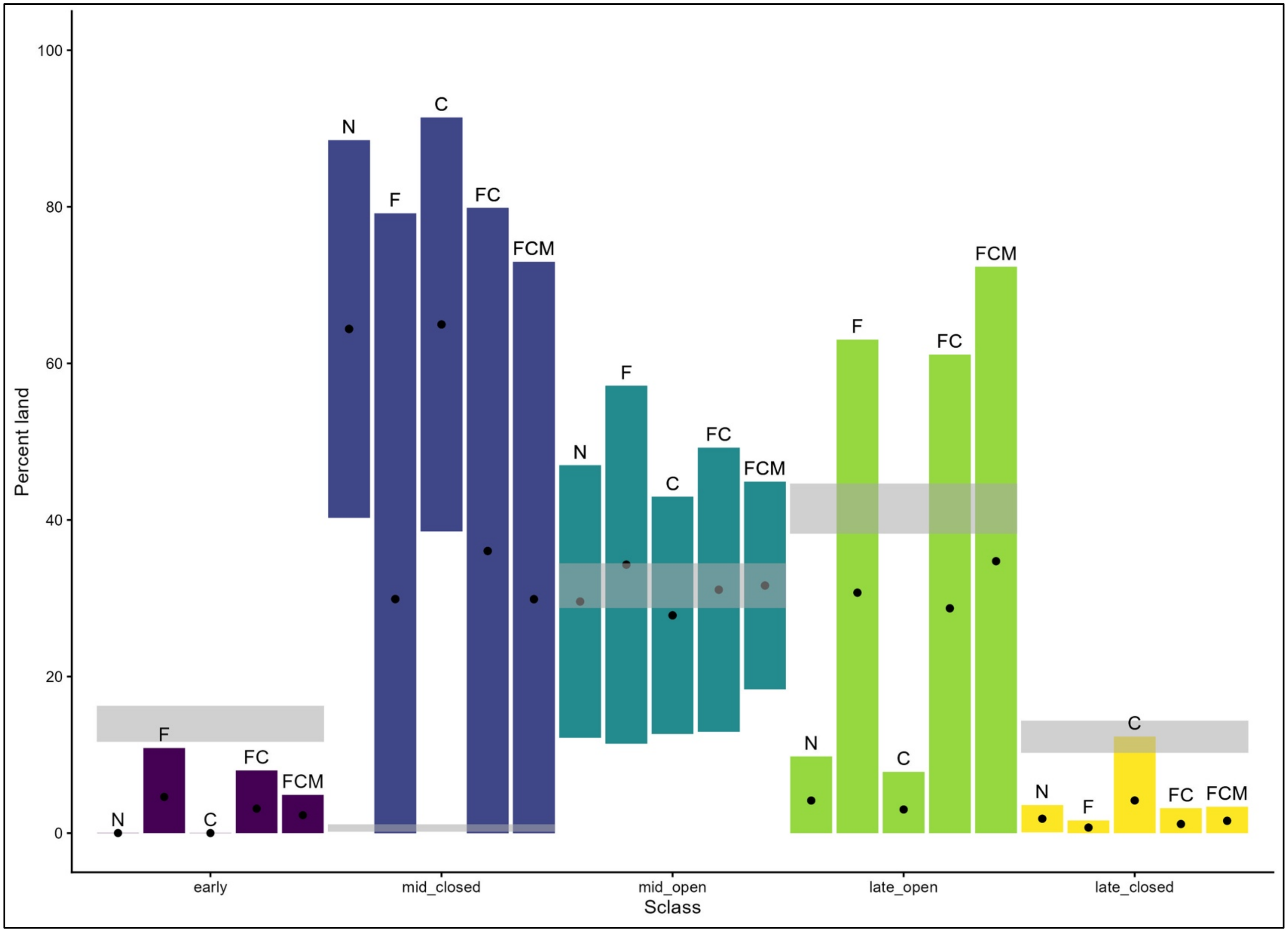

Figure 1.5 FRV of percent land in dry forests. Structure classes, in order of succession, are on the x-axis. Vertical bars represent the FRV ranges of each structure class. F = Fire, M = Management, C = Climate change. Black dots represent mean percent land. Horizontal grey bars represent Haugo et al. (2015) rRVs for dry mixed conifer forests.

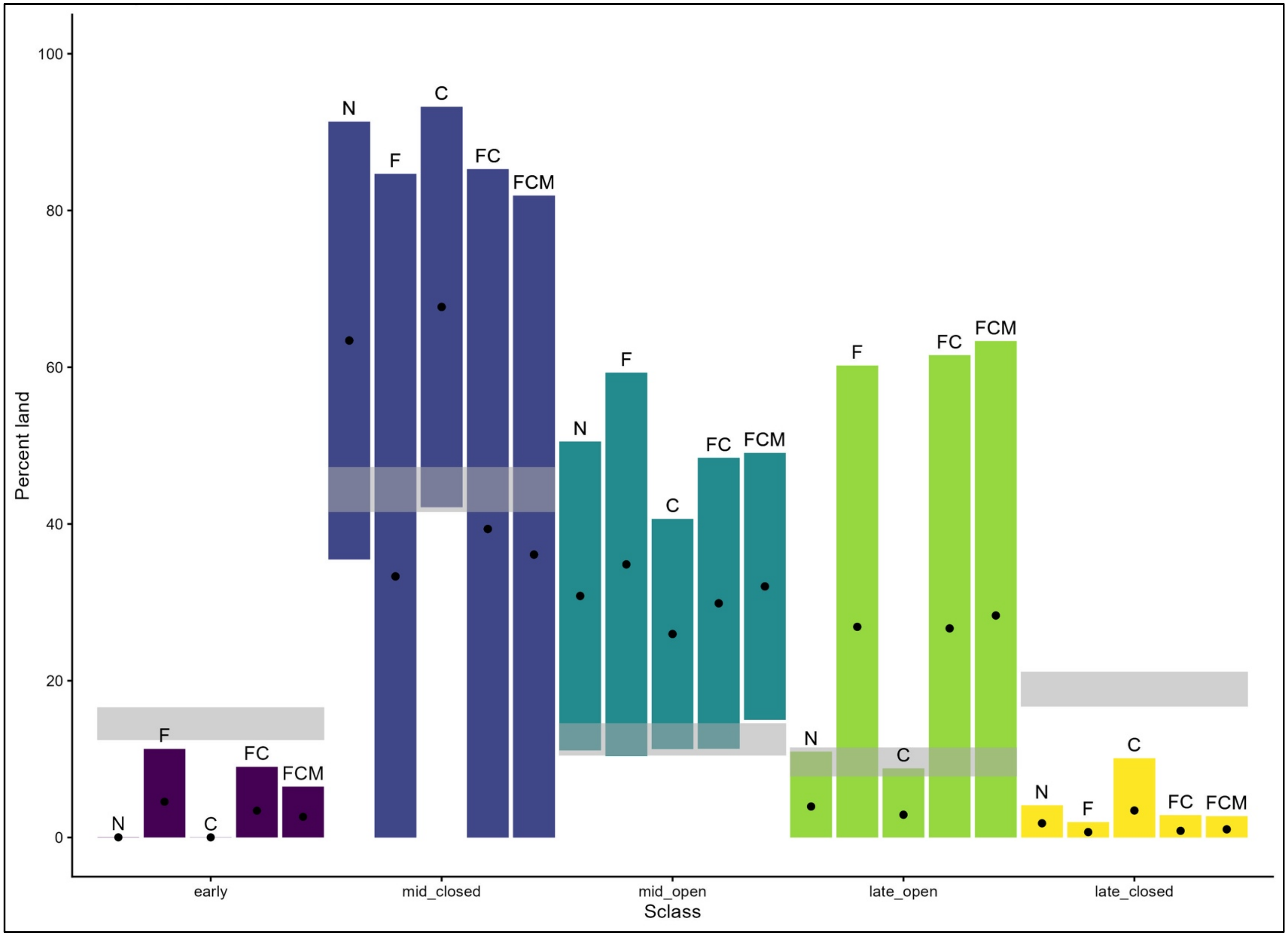

Figure 1.6 FRV of percent land in moist forests. Structure classes, in order of succession, are on the x-axis. Vertical bars represent the FRV ranges of each structure class. F = Fire, M = Management, C = Climate change. Black dots represent mean percent land. Horizontal grey bars represent Haugo et al. (2015) rRVs for moist mixed conifer forests.

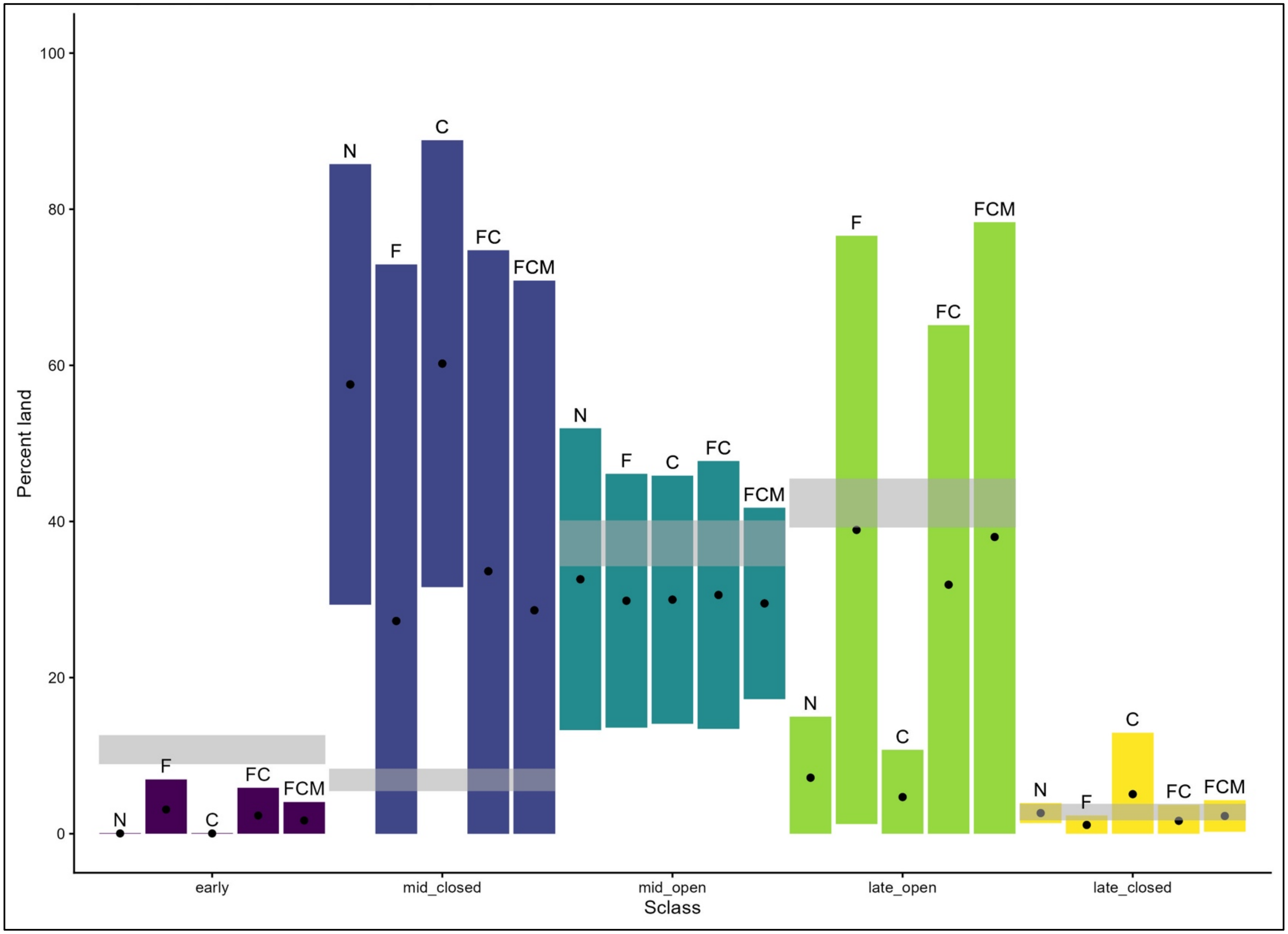

Figure 1.7 FRV of percent land in pipo, or ponderosa pine, forests. Structure classes, in order of succession, are on the x-axis. Vertical bars represent the FRV ranges of each structure class. F = Fire, M = Management, C = Climate change. Black dots represent mean percent land. Horizontal grey bars represent Haugo et al. (2015) rRVs for ponderosa pine forests.

4. Discussion

This study uses a process-based forest landscape and disturbance model to show how wildfire, climate change, and management can influence landscape composition and patterns of forest structure over the next century. This is also the first study to apply re-calibrated PNW parameters to a dry forest landscape to explore emergent and complex landscape patterns in this region. We found that 1) Wildfire reduced the percent cover, mean patch size, and patch density of mid-seral closed-canopy forest while increasing the percent cover and continuity of late seral, open canopy forests, and climate change increased the mean percent cover and continuity of closed canopy forests. 2) Management reduced the mean cover and continuity of mid-seral closed canopy forest, but the effect of management was a fraction of that of fire. 3) Despite wildfire and management reducing mid-seral closed canopy cover, the FRV of mid-seral closed canopy forest cover did not align with the rRV in any scenario in dry mixed conifer and ponderosa pine forests. The three key findings from this study have implications for management planning in a critical eastern Washington planning area and set a foundation of more questions to explore on this landscape using dynamic simulation modeling.

4.1 Effects of wildfire, climate change, and management

Low severity wildfire in eastern Washington dry to moist mixed conifer forests maintains late-seral, open canopy forest with large, fire-resistant trees and a low fuel profile that facilitates more low severity wildfire (Hessburg et al., 2005). Given that wildfire promoted the cover and continuity of late-seral open canopy forest, this implies that modeled low-severity wildfires opened the canopies of mid- and late-seral closed canopy forests while also reducing surface fuels and leaving large live legacy trees to persist. Further, wildfire caused a decrease in size and abundance (lower mean patch size, percent cover, and patch density) of mid-seral closed canopy patches as they were burned by wildfire or aged into late-seral closed-canopy forest. Increased abundance of open canopy forest and reduced abundance of mid-seral closed canopy forest patches has implications for management objectives across the Chumstick-LP planning area. In the context of wildfire risk reduction, increased fragmentation of closed canopy forest reduces the continuity of heavy fuels and limits the spread of high severity wildfire (Hessburg et al., 2005). When considering the implications for management of resilient forest structures, actions to facilitate more low severity and less high severity wildfire—fuel breaks, pre-fire density and fuel reduction treatments—can promote the beneficial effects of wildfire (Churchill et al., 2022).

Climate change increased the mean percent cover of closed canopy forest and reduced the mean percent cover of open canopy forest (when comparing climate change-only to the null, and when comparing wildfire and climate change to with wildfire-only). Looking closer at the species demographics in climate change scenarios compared to no-climate change scenarios, it can be deduced that climate change increased conifer productivity and, with fire enabled, facilitated ingrowth of deciduous broadleaf trees (Appendix A.8). This is explained by warmer temperature trends increasing tree and sapling conifer growth rates (possibly through increased growing degree days, reduced stress and mortality due to frost, increased overall productivity due to warmer average temperatures during the growing season) while simultaneously reducing conifer regeneration post-fire, possibly through increased seedling drought stress, or increased area burned by high severity wildfire due to increased overall live biomass (Davis et al., 2023; Harvey et al., 2016; Kemp et al., 2019).

Importantly, the wildfire module in iLand is dynamic, responding to changes in climate and fuel availability on the landscape. Modeled fire weather and fuel moisture deficit are determined by the Keetch-Byram Drought Index (KBDI), or a measure of soil and surface fuel moisture deficit due to drought (Seidl et al., 2014). The cumulative KBDI is calculated at each time step from each daily KBDI to determine the available fuel of each 1-ha pixel on the landscape, influencing the severity of wildfires burning through that pixel. Additionally, wildfire size is also determined by how each year's KBDI differs from the reference KBDI (Seidl et al., 2014). Thus, climate-induced changes in wildfire size, severity, and mean return interval may also explain the change in stem abundance from conifer- to broadleaf-dominated forest in portions of the landscape due to reduced conifer seedling survivorship and regeneration (Davis et al., 2023; Harvey et al., 2016; Kemp et al., 2019).

The role of management in reducing the mean percent cover and continuity of mid-seral closed canopy forest has implications for management planning in the Chumstick-LP planning area, as well as broadly for interior dry, vulnerable forests across the western USA. In the FCM simulation, deterministic management activities treated portions of the landscape with different levels of density and surface fuel reduction treatments (commercial thinning, noncommercial thinning, and maintenance surface fuel reduction) to open and disaggregate mid-seral closed canopy patches that may have initiated from dense regenerating broadleaf forest. However, the relative effect of management on forest structure was minimal compared to the effects of wildfire. This finding is consistent with contemporary assessments of the relative effect of beneficial wildfire on landscape-scale forest structure patterns compared to management efforts (Laughlin et al., 2023) and extends the implications of the effects of beneficial wildfire to the end of the century.

As climate change persists, post-fire environments are important areas of focus for mitigating vegetation transitions from dominance of fire-resilient conifer species (ponderosa pine) to resprouting deciduous broadleaf or shrub dominated forests (Meigs et al., 2023). More dynamic management—targeting forested areas dynamically in the simulation based on structure and species composition, post-fire management—or adjusting the map of operational filters—making certain areas available or unavailable for management—could further estimate the impact of management on the FRV of forest structure composition and pattern, and reflect more likely objectives and outcomes of management.

4.2 Comparing FRV with the rRV

Comparing the FRV with the rRV can inform how forests may change in response to specific drivers of change relative to refence ‘natural’, ‘healthy’, or ‘historical’ states. Comparisons of our simulated FRV with the Haugo et al. (2015) rRV informs how future forest conditions compare to estimates of dry to moist forest conditions undisturbed by wildfire suppression and exclusion and selective logging activity (Haugo et al., 2015).

Our finding that wildfire and management did not bring mean percent land of mid-seral closed canopy forest into the rRV range has implications for management planning in structurally departed forests across the region. Dry and pipo forests are in fire regime group 1 (Table 1.4), or they burn frequently (~0-35-year mean interval) under low severity fire conditions. A surplus of mid-seral closed canopy structure in these two dry/xeric forest types implies that there is still a deficit of wildfire disturbance in forests with a history of frequent low severity wildfire (Haugo et al., 2015), which is consistent with the finding from Donato et al.

(2023), that contemporary annual disturbance rates from wildfire and management (~36,000 ha/year) remain a fraction of historical annual disturbance rates (75,900 ha/year-92,200 ha/year) .

Percent cover of open canopy forests far exceeded the rRV range in moist mixed conifer forests, seemingly implying the opposite of dry forests—that there is too much fire creating more open canopy than is expected under the natural wildfire regime. Importantly, however, moist mixed conifer forests are in fire regime group 3 and—due to the lower frequency and more moderate severity of the characteristic fire regimes—should be assessed at a landscape level 2 scale (Table 1.4), or hydrologic unit code level 8 (~285,000ha) subbasins. In contrast, forests in fire regime group 1 should be assessed at the hydrologic unit code level 10 (~46,000ha) scale, which matches closely with the scale of the Chumstick-LP planning area (Haugo et al., 2015).

We found that there is less late seral forest across all FRV scenarios compared to the rRV in dry forests. There is also a deficit of late-seral open canopy structure and late-seral closed canopy structure in ponderosa pine and moist mixed conifer forests, respectively, compared to the rRV. This deficit in late seral forest across forest types could possibly be due to the short duration of the simulation—75 years—not giving trees enough time to grow into larger size classes. This outcome highlights the important role of management to allow for forests to grow into larger size classes without disturbance (land use change, logging, and high severity wildfire) and develop resistance to wildfire—thick bark, high self-pruned branches, mature cones for droppings seeds post-fire—that increase the likelihood of low severity wildfire and surviving biological legacies that facilitate the persistence of fire-prone forests (Haugo et al. 2015). Future simulation experiments could explore how much time it would take for contemporary forests to grow into larger diameter class, and where larger forests are more likely under future climate and wildfire conditions.

5. Limitations

5.1 Other agents of change

To assess effects of wildfire, climate, and management on landscape patterns of structure class, we excluded other drivers of forest change, such as pathogens, windfall, and development.

Thus, model outputs of forest change over the 75-year period *in silico* reflect less stochasticity than what is expected *in situ*.

5.2 Missing assessment of wildfire regime changes over time

As discussed, the wildfire module in iLand dynamically responds to changes in climate (Seidl et al., 2014). Thus, patterns of wildfire size, severity, and mean return interval likely varied across scenarios, but analyses of wildfire regime patterns fell out of the scope of this project. This is a pressing piece of the story that merits deeper exploration as a direct next step.

5.3 Source of high variability of mid-seral closed canopy structure

It is evident that mid-seral closed canopy forest had the most variability in percent land and mean patch size across all scenarios. When looking at the how forest structure changed in the simulation in the null model without any experimental drivers of change, the mean patch size of mid-seral closed canopy forest decreased early in the simulation as the cover of and continuity of mid-seral open canopy simultaneously began to increase. This could be due to high initial densities across the landscape and subsequent mortality due to competition for light and water, causing a quick reduction in closed canopy and gradual increase in other forest structure classes as succession played out.

5.4 Comparing FRV with Haugo et al. (2015) rRV

In this study, we compared our FRV results with the Haugo et al. (2015) rRVs, which are derived from modeled states of equilibrium under expected fire regimes. Haugo et al. (2015) used a state-and-transition model—a stochastic model of forest change between multiple possible states due to the expected rate and severity of fire disturbance—and a grid of 1,000 cells with an initial even distribution of each structure class. Authors ran ten simulations of 1000 years for each biophysical setting and used the last 500 years (structure class distributions reached a state of equilibrium by year 500) to inform the mean and ± 2SD range of structure class distributions for each rRV (n=5000). In contrast, our FRV of structure class distributions is derived from ten simulations of 75 annual timesteps (n=750)—one fifth of the number of data points used to generate the rRV. Moreover, our future climate change scenario FRVs induce a century-long trend of change in temperature and precipitation. To expect a state of equilibrium for the FRV would be contradictory to how we set up our model runs and overall experiment. Thus, the variability in the FRV is much higher than that of the rRV.

Additionally, a ubiquitous caveat for developing the rRV of pre-colonization conditions in most systems in colonized North America is a limited dataset of forest conditions before departure (Hessburg et al., 1999; Swetnam et al., 1999). Field-based reconstructions (e.g., tree-ring and fire scars) of climate and fire history provide evidence of disturbance and climate trends, though estimates of historical conditions based on these data are based on many assumptions (Swetnam et al., 1999). Aspatial statistical ranges and targets of the rRV are useful for a departure analysis on contemporary forests (Haugo et al., 2015), but do not provide information on the spatial dimension of historical conditions. In addition, climate data before the twentieth century is discontinuous (Swetnam et al., 1999), thus insufficient for adequate estimates of historical landscape-level dynamics before settler colonialism. Although the rRV is a useful reference against which to compare future projections of forest change, most reference conditions are incomplete in space or time. An opportunity for future improvement of this study would be to create structure class outputs using the 7-box scheme (Figure 1.1) for a 1:1 comparison of the FRV with rRV estimates of structure class patterns beyond percent land (mean patch size, patch density) at smaller scales that addresses smaller-scale (8-12,000ha) management planning at (Hessburg et al., 1999)

6. Conclusion

As climate and wildfire continue to change into the future, dry and moist mixed conifer forests are vulnerable to drought stress and uncharacteristic high severity wildfire. Since the later 20th century, scientists and managers have sought management solutions for restoring dry temperate forests affected by fire suppression, guided by a reference ‘historical’ or ‘natural’ range of variability of forest structure (Churchill et al., 2022; WADNR, 2025). However, aligning management strategies with possible future ranges of variability, which incorporate changing climate and wildfire regimes, is a key need for supporting forest resilience in the future (Keane et al., 2009). Results from this study show that wildfire disturbance may not be enough to reduce mid-seral closed canopy cover closer to reference ranges, and that management has a small influence the FRV of forest structure composition and pattern under future climate and wildfire scenarios by reducing and fragmenting the cover of mid-seral closed canopy forest.

These findings align with contemporary analyses of landscape-scale departure of forest structure (Laughlin et al., 2023) and wildfire disturbance (Donato et al., 2023) in eastern Washington. Comparisons of the FRV under future climate change, wildfire, and management scenarios with the rRV suggest that the overall need for restoration in dry forests of the PNW will persist to the end of the century, even while implementing density and fuel reduction treatments at 20-year rotations across the extent of feasibly treatable land. Further study is needed to explore how alternative adaptive management strategies influence the FRV.

Acknowledgements

This project was supported by funding from the USFS Region 6 Ecology Program (Grant 20-CS-11062754-057) and the USFS PNW Research Station and Wildfire Crisis Strategy (Grant 24-IA-11261925-115). Special thanks to support from the USFS Region 6 Ecology Office, former Region 6 ecologist Tom DeMeo, Skye Greenler, and Kerry Kemp for their collaborative work on this project. Thanks to Kristin Braziunas for guidance with using iLand and Jenna Morris for species calibration efforts. Thank you to WADNR ecologists Joshua S Halofsky and Ethan Hughes for input on calibrated species parameters and stand-level calibration benchmarks in eastern Washington. Thanks to Madison Laughlin for expertise and support with using the Haugo et al. (2015) rRV dataset, and Michele Buonanduci for expertise and support with collecting MTBS fire severity data for wildfire module calibration. Thanks to Tao Huang for friendly review of this document.

References

10-meter DEM files in the Wenatchee 1° by 2° quadrangle [WWW Document], n.d. URL https://gis.ess.washington.edu/data/raster/tenmeter/byquad/wenatchee/index.html (accessed 5.21.26).

20-Year Forest Health Strategic Plan: Eastern Washington | Department of Natural Resources [WWW Document], n.d. URL https://dnr.wa.gov/forest-resilience-division/forest-health-strategic-plans/20-year-forest-health-strategic-plan-eastern-washington (accessed 3.9.26).

Abatzoglou, J.T., Brown, T.J., 2012. A comparison of statistical downscaling methods suited for wildfire applications. International Journal of Climatology 32, 772–780. https://doi.org/10.1002/joc.2312

Agee, J., 1998. The Landscape Ecology of Western Forest Fire Regimes. Northwest Science 72, 24–34.

Braziunas, K.H., Hansen, W.D., Seidl, R., Rammer, W., Turner, M.G., 2018. Looking beyond the mean: Drivers of variability in postfire stand development of conifers in Greater Yellowstone. Forest Ecology and Management 430, 460–471. https://doi.org/10.1016/j.foreco.2018.08.034

CFLRP Proposals and Work Plans [WWW Document], n.d. URL https://www.fs.usda.gov/restoration/CFLRP/overview.shtml (accessed 5.13.24).

Churchill, D.J., Jeronimo, S.M.A., Hessburg, P.F., Cansler, C.A., Povak, N.A., Kane, V.R., Lutz, J.A., Larson, A.J., 2022. Post-fire landscape evaluations in Eastern Washington, USA: Assessing the work of contemporary wildfires. Forest Ecology and Management 504, 119796. https://doi.org/10.1016/j.foreco.2021.119796

Climate Toolbox [WWW Document], n.d. URL https://climatetoolbox.org/tool/Future-Boxplots (accessed 6.4.26)

Confronting the Wildfire Crisis: Initial Landscape Investments [WWW Document], 2022. . US Forest Service. URL https://www.fs.usda.gov/managing-land/wildfire-crisis/landscapes (accessed 5.13.24).

Coops, N.C., 2015. Characterizing Forest Growth and Productivity Using Remotely Sensed Data. Current Forestry Reports 1, 195–205. https://doi.org/10.1007/s40725-015-0020-x

Daum, K.L., Hansen, W.D., Gellman, J., Plantinga, A.J., Jones, C., Trugman, A.T., 2024. Do Vegetation Fuel Reduction Treatments Alter Forest Fire Severity and Carbon Stability in California Forests? Earth's Future 12, e2023EF003763. https://doi.org/10.1029/2023EF003763

Davis, K.T., Robles, M.D., Kemp, K.B., Higuera, P.E., Chapman, T., Metlen, K.L., Peeler, J.L., Rodman, K.C., Woolley, T., Addington, R.N., Buma, B.J., Cansler, C.A., Case, M.J., Collins, B.M., Coop, J.D., Dobrowski, S.Z., Gill, N.S., Haffey, C., Harris, L.B., Harvey, B.J., Haugo, R.D., Hurteau, M.D., Kulakowski, D., Littlefield, C.E., McCauley, L.A., Povak, N., Shive, K.L., Smith, E., Stevens, J.T., Stevens-Rumann, C.S., Taylor, A.H., Tepley, A.J., Young, D.J.N., Andrus, R.A., Battaglia, M.A., Berkey, J.K., Busby, S.U., Carlson, A.R., Chambers, M.E., Dodson, E.K., Donato, D.C., Downing, W.M., Fornwalt, P.J., Halofsky, J.S., Hoffman, A., Holz, A., Iniguez, J.M., Krawchuk, M.A., Kreider, M.R., Larson, A.J., Meigs, G.W., Roccaforte, J.P., Rother, M.T., Safford, H., Schaedel, M., Sibold, J.S., Singleton, M.P., Turner, M.G., Urza, A.K., Clark-Wolf, K.D., Yocom, L., Fontaine, J.B., Campbell, J.L., 2023. Reduced fire severity offers near-term buffer to climate-driven declines in conifer resilience across the western United States. Proceedings of the National Academy of Sciences 120, e2208120120. https://doi.org/10.1073/pnas.2208120120

DeMeo, T., Haugo, R., Ringo, C., Kertis, J., Acker, S., Simpson, M., Stern, M., 2018. Expanding Our Understanding of Forest Structural Restoration Needs in the Pacific Northwest. nwsc 92, 18–35. https://doi.org/10.3955/046.092.0104

Dollinger, C., Rammer, W., Suzuki, K.F., Braziunas, K.H., Keller, T.T., Kobayashi, Y., Mohr, J., Mori, A.S., Turner, M.G., Seidl, R., 2024. Beyond resilience: Responses to changing climate and disturbance regimes in temperate forest landscapes across the Northern Hemisphere. Global Change Biology 30, e17468. https://doi.org/10.1111/gcb.17468

Donato, D.C., Halofsky, J.S., Churchill, D.J., Haugo, R.D., Alina Cansler, C., Smith, A., Harvey, B.J., 2023. Does large area burned mean a bad fire year? Comparing contemporary wildfire years to historical fire regimes informs the restoration task in fire-dependent

forests. Forest Ecology and Management 546, 121372. https://doi.org/10.1016/j.foreco.2023.121372
Eidenshink, J., Schwind, B., Brewer, K., Zhu, Z.-L., Quayle, B., Howard, S., 2007. A Project for Monitoring Trends in Burn Severity. Fire Ecology 3, 3–21. https://doi.org/10.4996/fireecology.0301003
Franklin, J.F., Dyrness, C.T., 1973. Natural vegetation of Oregon and Washington. Gen. Tech. Rep. PNW-GTR-008. Portland, OR: U.S. Department of Agriculture, Forest Service, Pacific Northwest Research Station. 427 p 008.
Fraser, L.H., 2020. TRY—A plant trait database of databases. Global Change Biology 26, 189–190. https://doi.org/10.1111/gcb.14869
Furniss, T.J., Povak, N.A., Hessburg, P.F., Salter, R.B., Duan, Z., Wigmosta, M., 2023. Informing climate adaptation strategies using ecological simulation models and spatial decision support tools. Frontiers in Forests and Global Change 6. https://doi.org/10.3389/ffgc.2023.1269081
Gaudreau, J., Perez, L., Drapeau, P., 2016. BorealFireSim: A GIS-based cellular automata model of wildfires for the boreal forest of Quebec in a climate change paradigm. Ecological Informatics 32, 12–27. https://doi.org/10.1016/j.ecoinf.2015.12.006
Gray, A., Whittier, T.R., 2014. Carbon stocks and changes on Pacific Northwest national forests and the role of disturbance, management, and growth. Forest Ecology and Management. 328: 167-178 328, 167–178. https://doi.org/10.1016/j.foreco.2014.05.015
Gray, A., Whittier, T.R., Harmon, M.E., 2016. Carbon stocks and accumulation rates in Pacific Northwest forests: role of stand age, plant community, and productivity. Ecosphere 7, e01224. https://doi.org/10.1002/ecs2.1224
Gray, A.N., Brandeis, T.J., Shaw, J.D., McWilliams, W.H., Miles, P., 2012. Forest Inventory and Analysis Database of the United States of America (FIA). In: Dengler, J.; Oldeland, J.; Jansen, F.; Chytry, M.; Ewald, J., Finckh, M.; Glockler, F.; Lopez-Gonzalez, G.; Peet, R. K.; Schaminee, J .H. J., eds. Vegetation databases for the 21st century. Biodiversity and Ecology. 4: 225-231. 225–231. https://doi.org/10.7809/b-e.00079
Grimm, V., Revilla, E., Berger, U., Jeltsch, F., Mooij, W.M., Railsback, S.F., Thulke, H.-H., Weiner, J., Wiegand, T., DeAngelis, D.L., 2005. Pattern-Oriented Modeling of Agent-Based Complex Systems: Lessons from Ecology. Science 310, 987–991. https://doi.org/10.1126/science.1116681
Halofsky, J.E., Peterson, D.L., Harvey, B.J., 2020. Changing wildfire, changing forests: the effects of climate change on fire regimes and vegetation in the Pacific Northwest, USA. Fire Ecology 16, 4. https://doi.org/10.1186/s42408-019-0062-8
Halofsky, J.S., Halofsky, J.E., Burcsu, T., Hemstrom, M.A., 2014. Dry forest resilience varies under simulated climate-management scenarios in a central Oregon, USA landscape. Ecological Applications 24, 1908–1925. https://doi.org/10.1890/13-1653.1
Hansen, W.D., Abendroth, D., Rammer, W., Seidl, R., Turner, M.G., 2020. Can wildland fire management alter 21st-century subalpine fire and forests in Grand Teton National Park, Wyoming, USA? Ecological Applications 30, e02030. https://doi.org/10.1002/eap.2030
Hansen, W.D., Braziunas, K.H., Rammer, W., Seidl, R., Turner, M.G., 2018. It takes a few to tango: changing climate and fire regimes can cause regeneration failure of two subalpine conifers. Ecology 99, 966–977. https://doi.org/10.1002/ecy.2181
Harvey, B.J., Donato, D.C., Turner, M.G., 2016. High and dry: post-fire tree seedling establishment in subalpine forests decreases with post-fire drought and large stand-

replacing burn patches. Global Ecology and Biogeography 25, 655–669. https://doi.org/10.1111/geb.12443
Haugo, R., Zanger, C., DeMeo, T., Ringo, C., Shlisky, A., Blankenship, K., Simpson, M., Mellen-McLean, K., Kertis, J., Stern, M., 2015. A new approach to evaluate forest structure restoration needs across Oregon and Washington, USA. Forest Ecology and Management 335, 37–50. https://doi.org/10.1016/j.foreco.2014.09.014
Hessburg, P.F., Agee, J.K., Franklin, J.F., 2005. Dry forests and wildland fires of the inland Northwest USA: Contrasting the landscape ecology of the pre-settlement and modern eras. Forest Ecology and Management, Relative Risk Assessments for Decision –Making Related To Uncharacteristic Wildfire 211, 117–139. https://doi.org/10.1016/j.foreco.2005.02.016
Hessburg, P.F., Smith, B.G., Salter, R.B., 1999. Detecting Change in Forest Spatial Patterns from Reference Conditions. Ecological Applications 9, 1232–1252. https://doi.org/10.1890/1051-0761(1999)009%5B1232:DCIFSP%5D2.0.CO;2
Hesselbarth, M.H.K., Sciaini, M., With, K.A., Nowosad, J., 2019. landscapemetrics: an open-source R tool to calculate landscape metrics.
Holling, C.S., 1973. Resilience and Stability of Ecological Systems. Annual Review of Ecology, Evolution, and Systematics 4, 1–23. https://doi.org/10.1146/annurev.es.04.110173.000245
Johnston, J.D., 2017. Forest succession along a productivity gradient following fire exclusion. Forest Ecology and Management 392, 45–57. https://doi.org/10.1016/j.foreco.2017.02.050
Keane, R.E., Hessburg, P.F., Landres, P.B., Swanson, F.J., 2009. The use of historical range and variability (HRV) in landscape management. Forest Ecology and Management 258, 1025–1037. https://doi.org/10.1016/j.foreco.2009.05.035
Keane, R.E., Holsinger, L.M., Loehman, R., 2020. Bioclimatic modeling of potential vegetation types as an alternative to species distribution models for projecting plant species shifts under changing climates. Forest Ecology and Management 477, 118498. https://doi.org/10.1016/j.foreco.2020.118498
Keane, R.E., Loehman, R.A., Holsinger, L.M., 2019. Selecting a Landscape Model for Natural Resource Management Applications. Current Landscape Ecology Reports 4, 31–40. https://doi.org/10.1007/s40823-019-00036-6
Kemp, K.B., Higuera, P.E., Morgan, P., Abatzoglou, J.T., 2019. Climate will increasingly determine post-fire tree regeneration success in low-elevation forests, Northern Rockies, USA. Ecosphere 10, e02568. https://doi.org/10.1002/ecs2.2568
Kruszka, S.S., Morris, J.E., Seidl, R., Hansen, W.D., Simensen, T., Turner, M.G., Braziunas, K.H., Harvey, B.J., *In Prep*. Calibrated tree species parameters to operationalize the forest landscape simulation model iLand for the Pacific Northwest, USA. Data in Brief.
Landres, P.B., Morgan, P., Swanson, F.J., 1999. Overview of the Use of Natural Variability Concepts in Managing Ecological Systems. Ecological Applications 9, 1179–1188. https://doi.org/10.2307/2641389
Laughlin, D.C., Bakker, J.D., Stoddard, M.T., Daniels, M.L., Springer, J.D., Gildar, C.N., Green, A.M., Covington, W.W., 2004. Toward reference conditions: wildfire effects on flora in an old-growth ponderosa pine forest. Forest Ecology and Management 199, 137–152. https://doi.org/10.1016/j.foreco.2004.05.034

Laughlin, M.M., Bakker, J.D., Churchill, D.J., Gregory, M.J., DeMeo, T., Alvarado, E.C., Harvey, B.J., 2023. Trends in forest structure restoration need over three decades with increasing wildfire activity in the interior Pacific Northwest US. Forest Ecology and Management 527, 120607. https://doi.org/10.1016/j.foreco.2022.120607

Lillybridge, T.R., Kovalchik, B.L., Williams, C.K., Smith, B.G., 1995. Field guide for forested plant associations of the Wenatchee National Forest. Gen. Tech. Rep. PNW-GTR-359. Portland, OR: U.S. Department of Agriculture, Forest Service, Pacific Northwest Research Station. 335 p. In cooperation with: Pacific Northwest Region, Wenatchee National Forest 359. https://doi.org/10.2737/PNW-GTR-359

Meigs, G.W., Case, M.J., Churchill, D.J., Hersey, C.M., Jeronimo, S.M.A., Smith, L.A.C., 2023. Drought, wildfire and forest transformation: characterizing trailing edge forests in the eastern Cascade Range, Washington, USA. Forestry (Lond) 96, 340–354. https://doi.org/10.1093/forestry/cpac046

Miller, D.A., White, R.A., 1998. A conterminous United States multilayer soil characteristics dataset for regional climate and hydrology modeling. Earth Interactions 2, 1–26. https://doi.org/10.1175/1087-3562(1998)002%3C0001:ACUSMS%3E2.3.CO;2

Radcliffe, D.C., Bakker, J.D., Churchill, D.J., Alvarado, E.C., Peterson, D.W., Laughlin, M.M., Harvey, B.J., 2024. How are long-term stand structure, fuel profiles, and potential fire behavior affected by fuel treatment type and intensity in Interior Pacific Northwest forests? Forest Ecology and Management 553, 121594. https://doi.org/10.1016/j.foreco.2023.121594

Raymond, C.L., McKenzie, D., 2013. Temporal carbon dynamics of forests in Washington, US: Implications for ecological theory and carbon management. Forest Ecology and Management 310, 796–811. https://doi.org/10.1016/j.foreco.2013.09.026

Richmond, T., 2024. Chumstick to LP Restoration Project Landscape Evaluation and Prescription. Resilient Forestry.

Riley, K.L., Grenfell, I.C., Shaw, J.D., Finney, M.A., 2022. TreeMap 2016 Dataset Generates CONUS-Wide Maps of Forest Characteristics Including Live Basal Area, Aboveground Carbon, and Number of Trees per Acre. j for 120, 607–632. https://doi.org/10.1093/jofore/fvac022

Rollins, M.G., 2009. LANDFIRE: a nationally consistent vegetation, wildland fire, and fuel assessment. International Journal of Wildland Fire 18, 235–249. https://doi.org/10.1071/WF08088

Seidl, R., Rammer, W., Scheller, R.M., Spies, T.A., 2012a. An individual-based process model to simulate landscape-scale forest ecosystem dynamics. Ecological Modelling 231, 87–100. https://doi.org/10.1016/j.ecolmodel.2012.02.015

Seidl, R., Rammer, W., Spies, T.A., 2014. Disturbance legacies increase the resilience of forest ecosystem structure, composition, and functioning. Ecological Applications 24, 2063–2077. https://doi.org/10.1890/14-0255.1

Seidl, R., Spies, T.A., Rammer, W., Steel, E.A., Pabst, R.J., Olsen, K., 2012b. Multi-scale Drivers of Spatial Variation in Old-Growth Forest Carbon Density Disentangled with Lidar and an Individual-Based Landscape Model. Ecosystems 15, 1321–1335. https://doi.org/10.1007/s10021-012-9587-2

Smithwick, E.A.H., Harmon, M.E., Remillard, S.M., Acker, S.A., Franklin, J.F., 2002. Potential Upper Bounds of Carbon Stores in Forests of the Pacific Northwest. Ecological

Applications 12, 1303–1317. https://doi.org/10.1890/1051-0761(2002)012%5B1303:PUBOCS%5D2.0.CO;2
Swetnam, T.W., Allen, C.D., Betancourt, J.L., 1999. Applied Historical Ecology: Using the Past to Manage for the Future. Ecological Applications 9, 1189–1206. https://doi.org/10.1890/1051-0761(1999)009%5B1189:AHEUTP%5D2.0.CO;2
Thom, D., Rammer, W., Albrich, K., Braziunas, K.H., Dobor, L., Dollinger, C., Hansen, W.D., Harvey, B.J., Hlásny, T., Hoecker, T.J., Honkaniemi, J., Keeton, W.S., Kobayashi, Y., Kruszka, S.S., Mori, A., Morris, J.E., Peters-Collaer, S., Ratajczak, Z., Simensen, T., Storms, I., Suzuki, K.F., Taylor, A.R., Turner, M.G., Willis, S., Seidl, R., 2024. Parameters of 150 temperate and boreal tree species and provenances for an individual-based forest landscape and disturbance model. Data in Brief 55, 110662. https://doi.org/10.1016/j.dib.2024.110662
Turner, M.G., Braziunas, K.H., Hansen, W.D., Hoecker, T.J., Rammer, W., Ratajczak, Z., Westerling, A.L., Seidl, R., 2022a. The magnitude, direction, and tempo of forest change in Greater Yellowstone in a warmer world with more fire. Ecological Monographs 92, e01485. https://doi.org/10.1002/ecm.1485
Turner, M.G., Seidl, R., 2023. Novel Disturbance Regimes and Ecological Responses. Annual Review of Ecology, Evolution, and Systematics 54, 63–83. https://doi.org/10.1146/annurev-ecolsys-110421-101120
WADNR, 2020. Forest health assessment and treatment framework (RCW 76.06.200), Washington State Department of Natural Resources. Olympia, WA.
WADNR, 2025. Wildfire Season 2024 - Work of Wildfire Assessment. Washington State Department of Natural Resources, Olympia, WA.
Welty, J., Jeffries, M., 2021. Combined wildland fire datasets for the United States and certain territories, 1800s-Present. U.S. Geological Survey data release. https://doi.org/10.5066/P9ZXGFY3

Appendix A.1 Structure class schemes across management agencies in Washington (WADNR, 2020). The 5-box (Colville NF) model was used in this study and has been applied to forests across the entire region. The 6-box model is used in the WADNR Forest health treatment summary table (Figure 1.1)

Table 6: Structure classes used for planning areas.

LiDAR/DAP 8 Classes	6 Classes	Colville NF 5 Classes	Definition	Corresponding Structure Classes from Photo-Interpretation System
Small Open	Small Open	Early	canopy cover[1] < 10% OR dbh[2] < 10″, canopy cover ≥ 10% dbh and < 40%	Stand Initiation
Small Closed	Small Dense	Early	dbh < 10", canopy cover ≥ 40%	Stand Initiation; Stem exclusion closed canopy
Medium Open	Medium Open	Mid Open	dbh ≥ 10″ and < 20″, canopy cover ≥ 10% and < 40%	Stem exclusion open canopy
Medium Moderate	Medium Dense	Mid Closed	dbh ≥ 10″ and < 20″, canopy cover ≥ 40% and < 60%	Young forest multistory; understory re-initiation; Stem exclusion closed canopy
Medium Closed	Medium Dense	Mid Closed	dbh ≥ 10" and < 20", canopy cover ≥ 60%	
Large Open	Large Open	Late Open	dbh ≥ 20", canopy cover ≥ 10% and < 40%	Old forest single story; Stem exclusion open canopy
Large Moderate	Large Dense	Late Closed	dbh ≥ 20", canopy cover ≥ 40% and < 60%	Old forest multistory; young forest multistory
Large Closed	Large Dense	Late Closed	dbh ≥ 20", canopy cover ≥ 60%	

[1] Canopy cover is derived from LiDAR or DAP using the percent of returns above 6.6 feet.
[2] Tree diameter at breast height (DBH) was derived from modeling relationships between LiDAR or DAP tree height layers and tree diameter from field plots. Tree diameter used to define structure class is based on the mean diameter of the dominant and co-dominant trees in a field plot. It is calculated by deriving the quadratic mean diameter of trees whose diameters are in the top 25% of trees that are greater than 5" in diameter.

Appendix A.2 Area covered by dry, moist, and pipo forest (or biophysical setting) across Chumstick-LP planning area.

Extent	total area (ha)	Dry area (ha)	Dry % of total	Moist area (ha)	Moist % of total	Pipo area (ha)	Pipo % of total	Other area (ha)	Other % of total
Chumstick Creek	12194	5599	45.9	4885	40.1	1542	12.6	168	1.4
Eagle Creek	7050	4605	65.3	1353	19.2	1027	14.6	65	0.9
Derby Canyon-Wenatchee River	5569	2840	51.0	753	13.5	1933	34.7	43	0.8
Ollala Canyon-Wenatchee River	4560	2408	52.8	207	4.5	1945	42.7	0	0.0
Lower Peshastin Creek	9027	4418	48.9	1786	19.8	1993	22.1	830	9.2
Full landscape	38400	19870	51.7	8984	23.4	8440	22.0	1106	2.9

Appendix A.3.1 Wildfire module calibration: iLand vs. observed proportion of low, moderate, and high severity

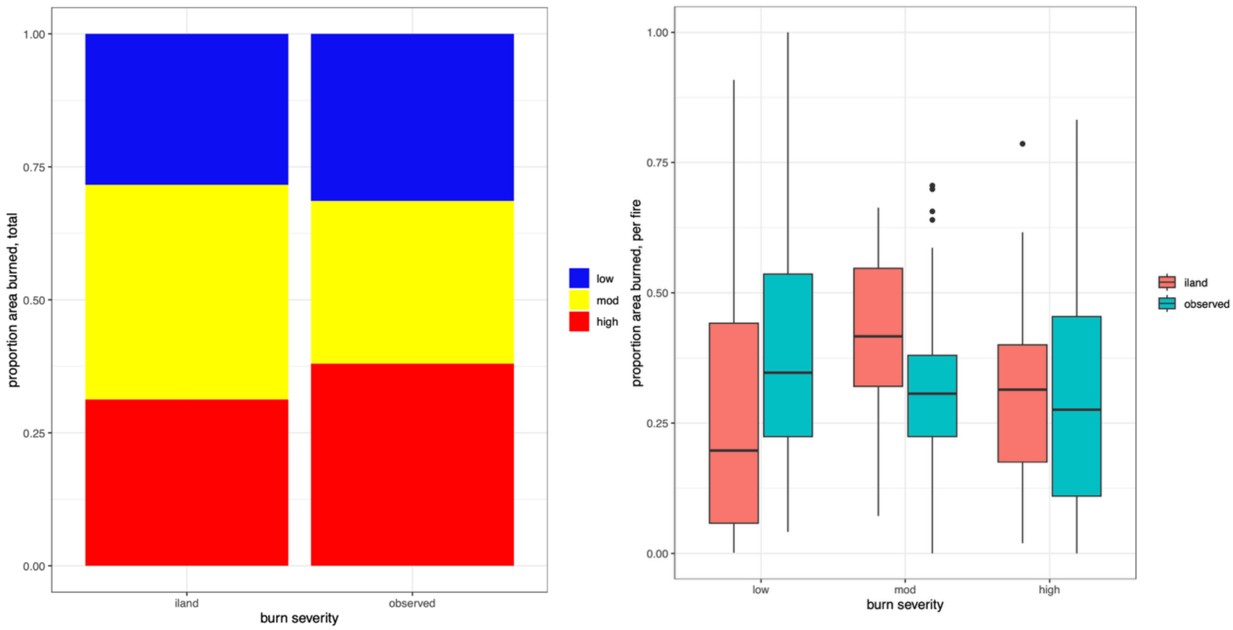

Appendix A.3.2 Wildfire module calibration: iLand vs observed total area burned (left) and burn probability (right)

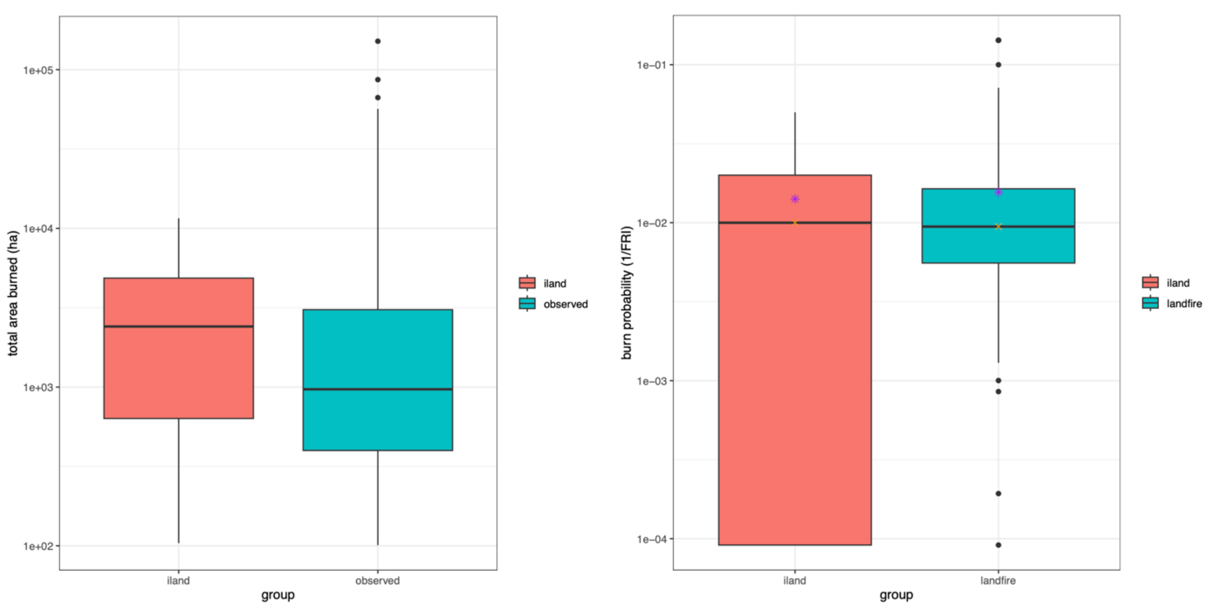

Appendix A.3.3 Wildfire module calibration: default and calibrated parameters for iLand's dynamic wildfire module. Default parameters correspond to those originally calibrated for the western cascades of Oregon (Seidl et al., 2014). Other wildfire parameters that more directly draw from the wildfire record for a specific spatial extent (e.g. averageFireSize, minFireSize) do not have default values (NA).

Parameter name	Unit	Default	Calibrated
averageFireSize	ha	NA	4067
minFireSize	ha	NA	0.04
maxFireSize	ha	NA	414500
fireReturnInterval	year	NA	40
fireExtinctionProbability	dim.	0	0.12
crownKill1	dim.	0.2111	0.18
crownKill2	dim.	-0.00445	-0.0044
crownKillDbh	cm	40	40

Appendix A.4.1 Carbon calibration: aboveground carbon pools chronosequence for dry E. Cascades forests.

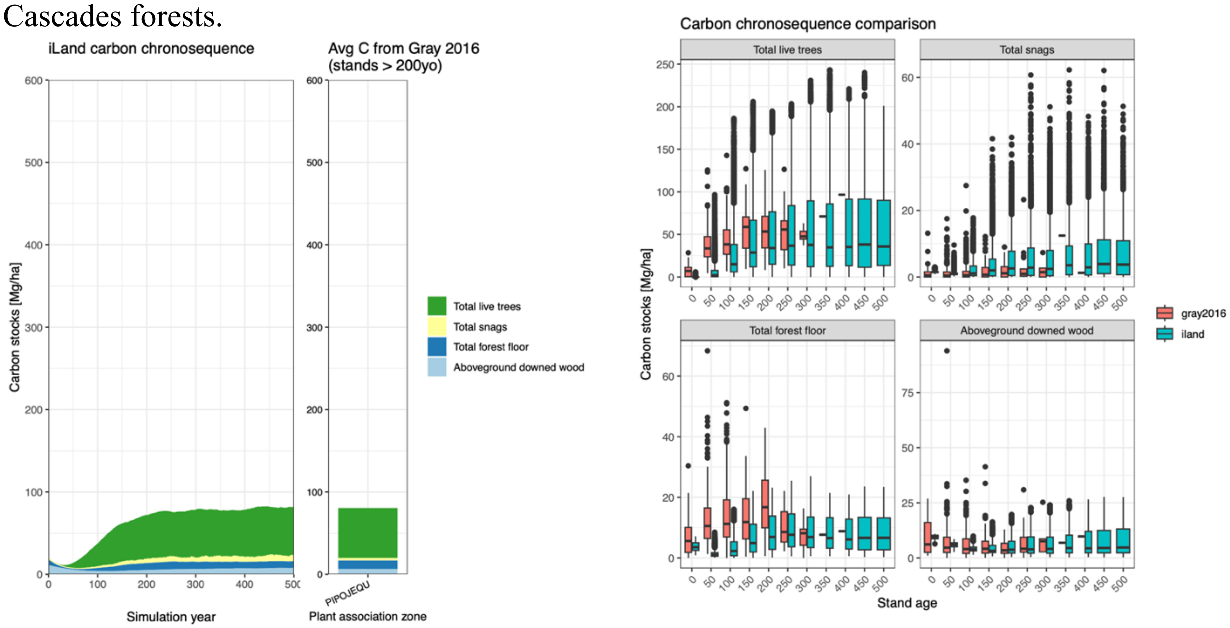

Appendix A.4.2 Carbon calibration: soil carbon and total carbon chronosequence for dry E. Cascades forests.

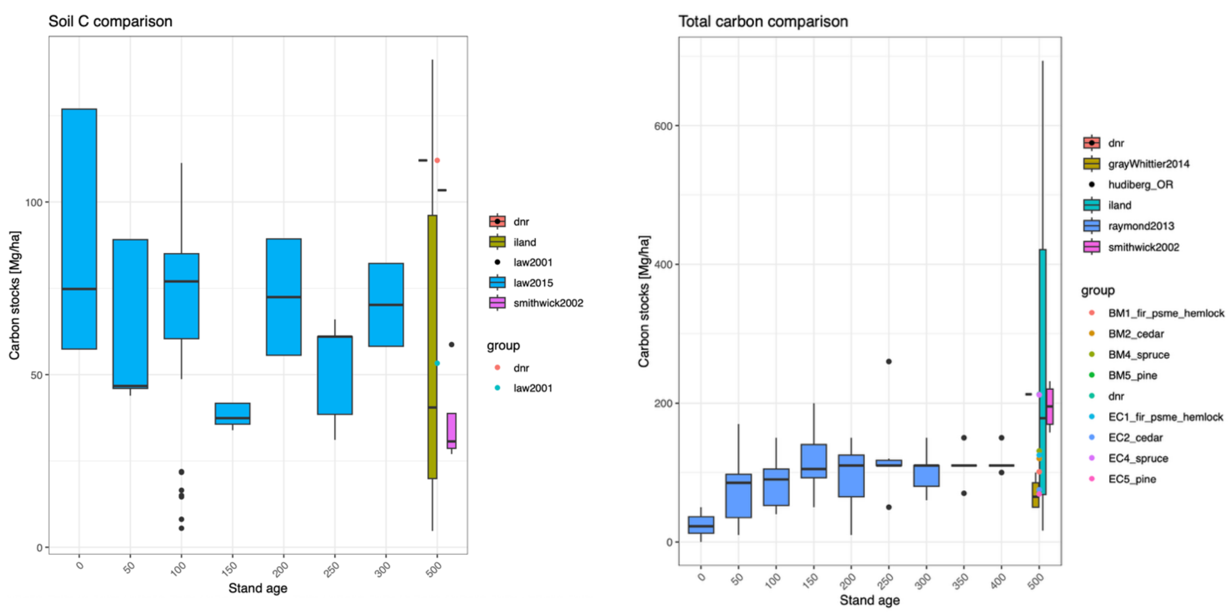

Appendix A.4.3 Species-specific parameters for rates of snag decay (snagKWS), snag half life (snagHalfLife), litter/small branch decay (snagKYL), and downed woody debris decay (snagKYR).

Species	shortName	snagKSW	snagHalfLife	snagKYL	snagKYR
western white pine	pimo	0.009	32	0.24	0.031
lodgepole pine	pico	0.132	8	0.2	0.021
Engelmann spruce	pien	0.114	12	0.243	0.033
subalpine fir	abla	0.276	15	0.373	0.045
quaking aspen	potr	0.247	7	0.198	0.164
ponderosa pine	pipo	0.806	10	0.082	0.056
western larch	laoc	0.054	30	0.179	0.044
subalpine larch	laly	0.016	16	0.359	0.031
Sitka spruce	pisi	0.034	12	0.189	0.038
red alder	alru	0.108	7	0.218	0.123
Alaska yellow-cedar	cano	0.029	30	0.335	0.018
black cottonwood	poba	0.108	7	0.218	0.123
Pacific dogwood	conu	0.108	7	0.218	0.123
western redcedar	thpl	0.029	30	0.184	0.018
western hemlock	tshe	0.061	20	0.189	0.038
grand fir	abgr	0.02	15	0.3	0.101
whitebark pine	pial	0.016	32	0.359	0.031
noble fir	abpr	0.058	20	0.238	0.066
Pacific silver fir	abam	0.058	15	0.238	0.066
mountain hemlock	tsme	0.084	12	0.446	0.126
bigleaf maple	acma	0.108	7	0.218	0.123
coastal Douglas-fir	psmem	0.086	30	0.129	0.031
Pacific yew	tabr	0.016	16	0.224	0.018
bitter cherry	prem	0.108	7	0.218	0.123
golden chinquapin	chch	0.058	7	0.195	0.066

Appendix A.4.4 Default constants of soil organic matter decomposition and soil humification rates

Constants	
som_decomp	0.0343
soil_humification	0.368

Appendix A.5.1 Landscape evaluation: basal area by species

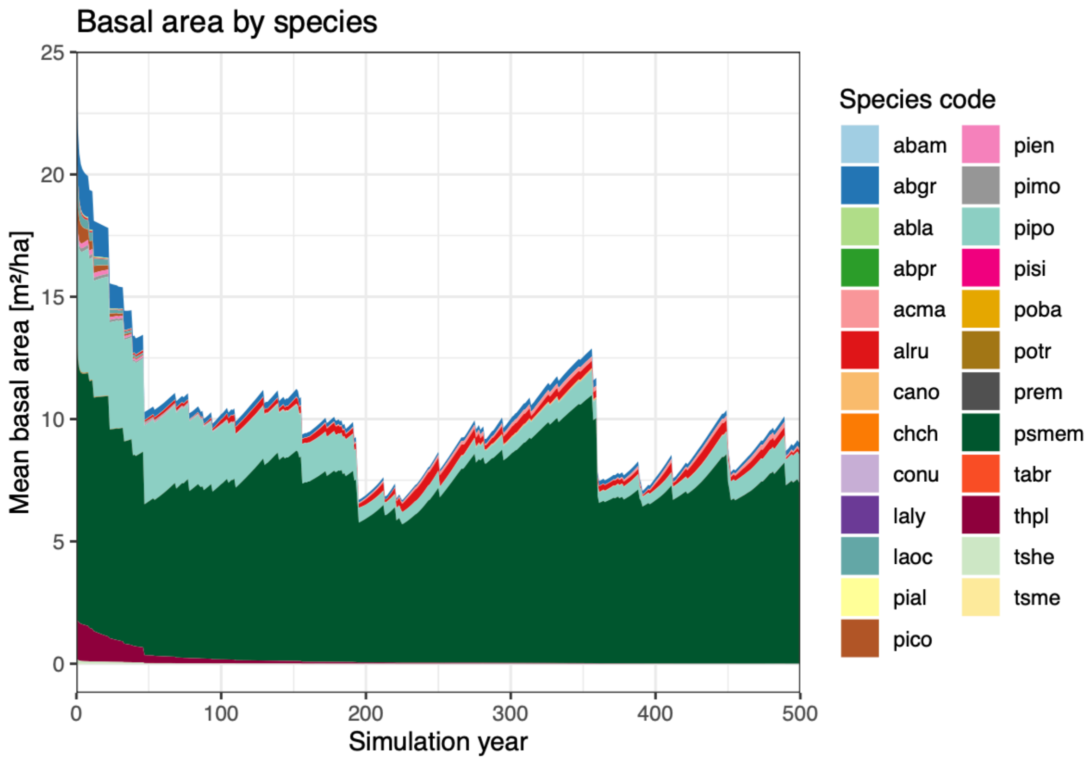

Appendix A.5.2 Basal area by species across elevation

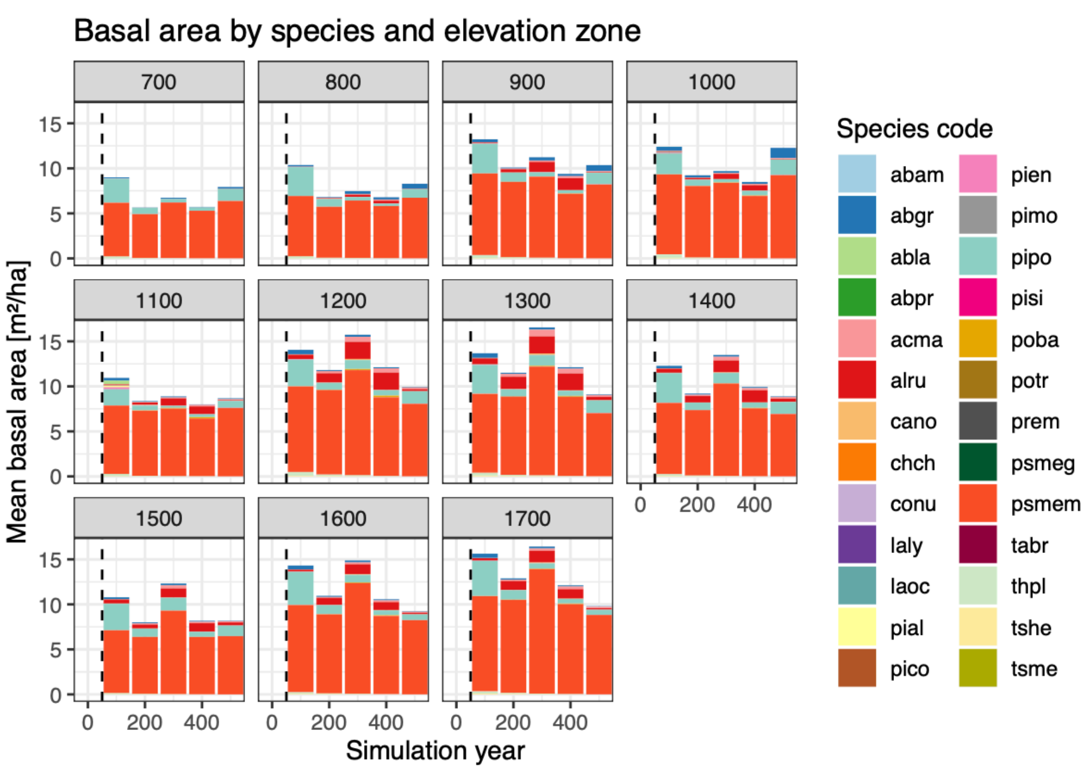

Appendix A.5.3 Landscape evaluation: aboveground carbon pools over time

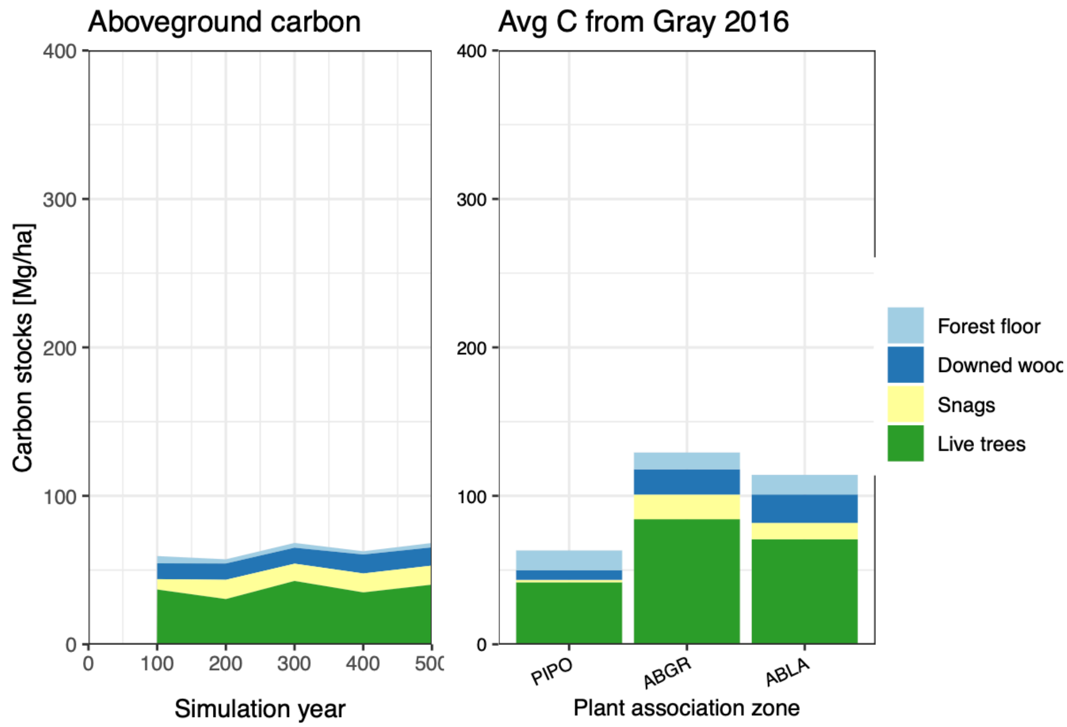

Appendix A.5.4 Landscape evaluation: aboveground carbon pools over elevation

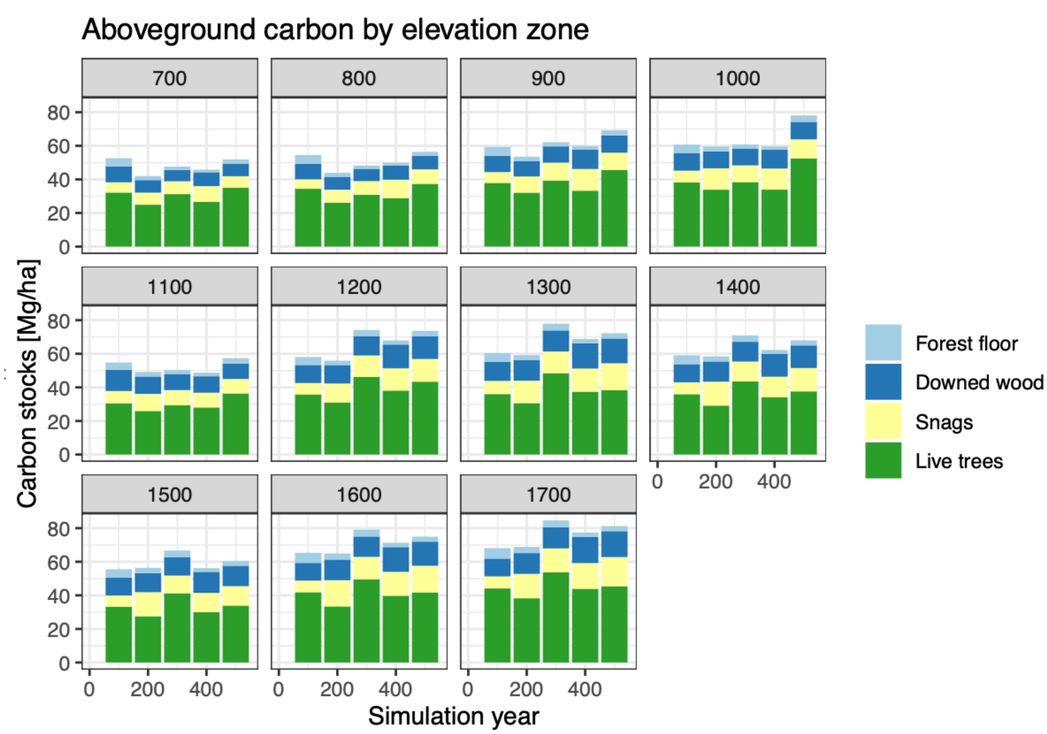

Appendix A.6.1 Landscape-level management schedule sensitivity analysis results: fire disabled. a = 1/2 of the landscape treated every ten years, b = 1/4 every five, c = 1/5 every four, d = 1/20 every year. This study uses schedule c.

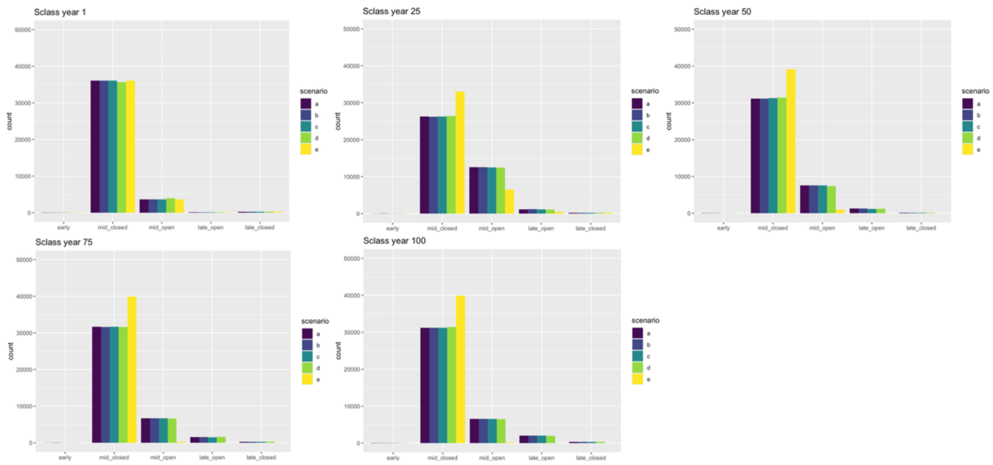

Appendix A.6.2 Landscape-level management schedule sensitivity analysis results: fire enabled. a = 1/2 of the landscape treated every ten years, b = 1/4 every five, c = 1/5 every four, d = 1/20 every year. This study uses schedule c.

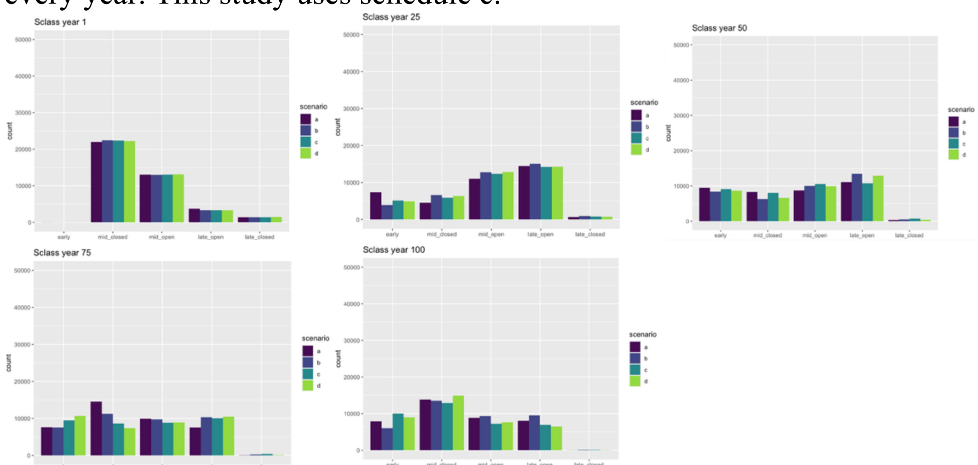

Appendix A.7.1 Transition matrix of structure class transitions one year pre-management (rows) and one year post-management (columns) across all managed pixels using original structure class definitions.

	Early	Mid-Closed	Mid-Open	Late-Open	Late-Closed
Early	687	911	2562	66	7
Mid-Closed	1	2517	4383	457	125
Mid-Open	6	16	1021	36	0
Late-Open	0	0	3	41	0
Late-Closed	0	0	0	48	31

Appendix A.7.2 Transition matrix of structure class transitions one year pre-management (rows) and one year post-management (columns) across all managed pixels using adjusted structure class definitions.

	Early	Mid-Closed	Mid-Open	Late-Open	Late-Closed
Early	1	0	3	0	0
Mid-Closed	0	3669	6900	521	132
Mid-Open	0	38	1493	38	0
Late-Open	0	0	3	41	0
Late-Closed	0	0	0	48	31

Appendix A.7.3 Sankey diagrams of structure class transitions one year pre-management and one year post-management across all managed pixels using original and adjusted structure class definitions.

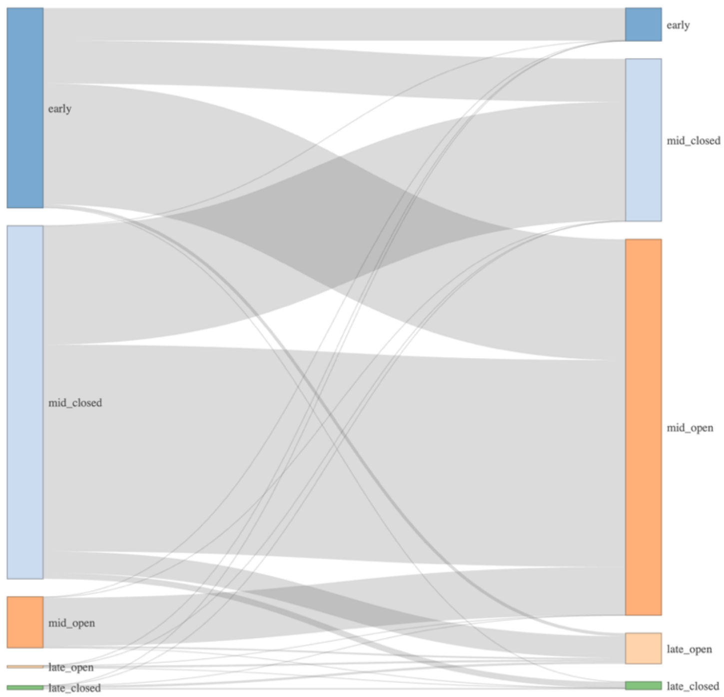

Sankey diagram of one year pre- and post- management with original structure class definitions

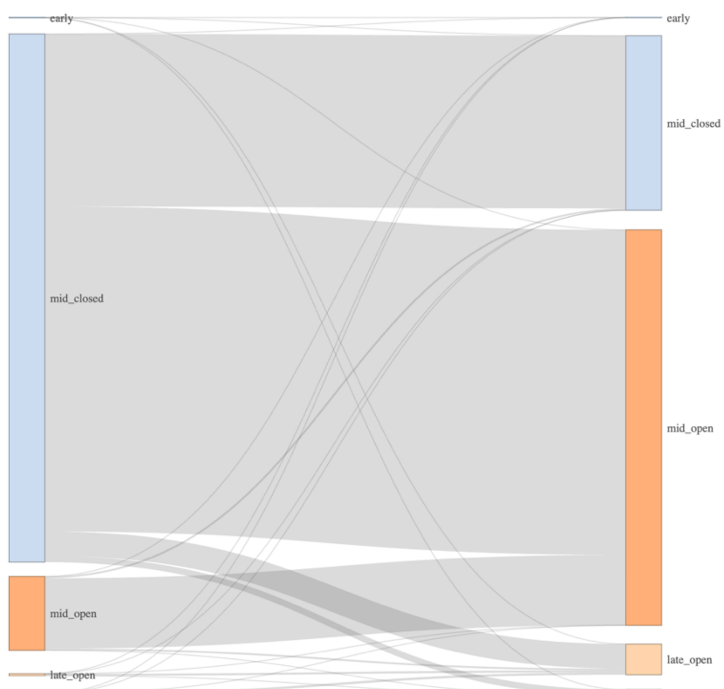

Sankey diagram of one year pre- and post- management with adjusted structure class definitions

Appendix A.7.4 Maps of structure class transitions one year pre-management and one year post-management across all managed pixels using original and adjusted structure class definitions.

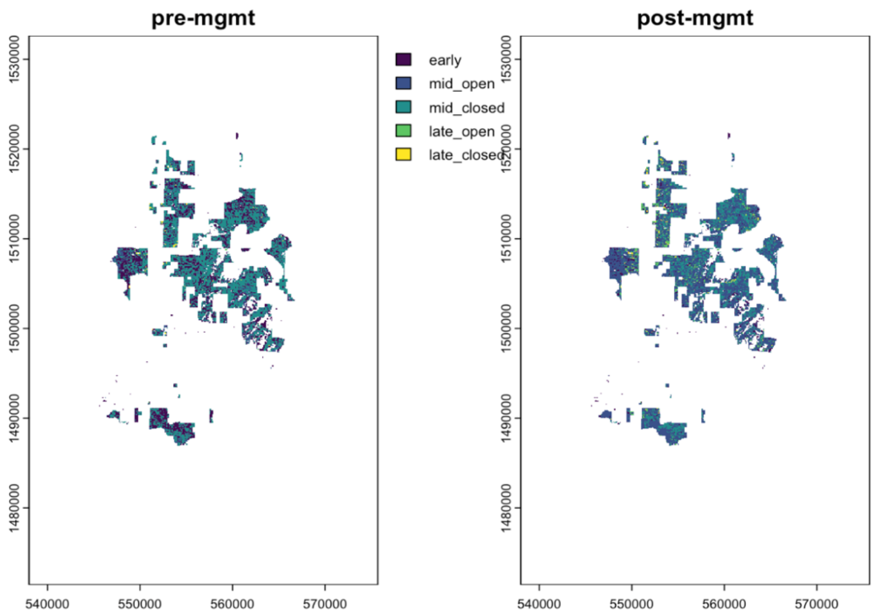

Sankey diagram of one year pre- and post-management with original structure class definitions

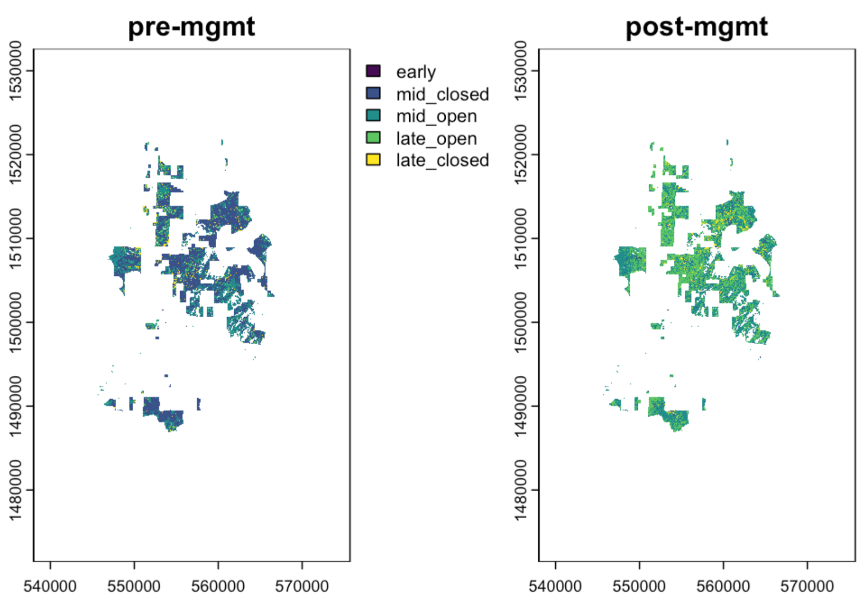

Sankey diagram of one year pre- and post-management with adjusted structure class definitions

Appendix A.8 Broadleaf and deciduous density, diameter, and volume trajectories across the entire landscape for experiments 8 (null), 1 (F), 3 (C), 5 (FC), and 4 (FCM).